arXiv:hep-ph/0311304v3 14 May 2004

YITP-SB-03-58

# NNLO corrections to massive lepton-pair production in longitudinally polarized proton-proton collisions

V. Ravindran
*Harish-Chandra Research Institute,*
*Chhatnag Road, Jhusi,*
*Allahabad, 211019, India.*

J. Smith [1]
*C.N. Yang Institute for Theoretical Physics,*
*State University of New York at Stony Brook, New York 11794-3840, USA.*

W.L. van Neerven
*Instituut-Lorentz*
*University of Leiden,*
*PO Box 9506, 2300 RA Leiden,*
*The Netherlands.*

October 2003

**Abstract**

We present the full next-to-next-to-leading order (NNLO) coefficient functions for the polarized cross section $d\Delta\sigma/dQ$ for the Drell-Yan process $p+p \to l^+l^- +' X'$. Here $'X'$ denotes any inclusive hadronic state and $Q$ represents the invariant mass of the lepton pair. All QCD partonic subprocesses have been included provided the lepton pair is created by a virtual photon, which is a valid approximation for $Q < 50$ GeV. Unlike the differential distribution w.r.t. transverse momentum the dominant subprocess for the integrated cross section is given by $q + \bar{q} \to \gamma^* +' X'$ and its higher order corrections so that massive lepton pair production provides us with an excellent tool to measure the polarized anti-quark densities. Our calculations are carried out using the method of $n$-dimensional regularization by making a special choice for the $\gamma_5$ matrix. We give predictions for double longitudinal spin asymmetry measurements at the RHIC.

PACS numbers: 12.38.Bx, 12.38.Qk, 13.85.Qk

[1]partially supported by the National Science Foundation grant PHY-0098527.

# 1 Introduction

With the advent of the RHIC at BNL we have a new facility to study the spin structure of the proton, (for a review on the potential of the RHIC see [1]), which supplements the existing polarized lepton-hadron machines. Polarized proton-proton collisions with a very high luminosity and a maximum centre of mass energy of $\sqrt{s} = 500$ GeV will provide us with many more details about spin distributions than possible with the existing lepton-hadron machines, which give very little information about the polarized gluon and sea-quark parton densities. If we limit ourselves to the Drell-Yan process where the initial state hadrons are longitudinally polarized then the gluon initiated subprocess dominates the quark process in $d^3\Delta\sigma/dQ^2/dy/dp_T$ at a transverse momentum $p_T > Q/2$ and fixed rapidity $y$ [2], [3]. This result, however, depends on the parton densities involved. For a study of the cross section $d^3\Delta\sigma/dQ^2/dy/dp_T$ and its dependence on the parton density set we refer to the complete NLO calculation in [4] (the non-singlet part was already done in [5] and [6]). However for the totally integrated cross section $d\Delta\sigma/dQ$ and for $p + p \to l^+l^- + `X'$ the sea quark initiated process dominates the reaction for the whole phase space. Therefore this process provides us with an excellent tool to measure the sea-quark densities. This process was calculated up to next-to-leading order (NLO) in [7] and subsequently confirmed in [8], [9] [10] and [11]. It is our goal to add all subprocesses which appear in the next-to-next-to-leading order (NNLO) contribution to $d\Delta\sigma/dQ$ and to see whether the sea quark dominance persists. In order to calculate such a process one has first to specify the scheme for the $\gamma_5$ matrix if one wants to use $n$-dimensional regularization and massless quarks. In this paper we use the HVBM prescription of 't Hooft and Veltman [12] which is more elaborated upon by Breitenlohner and Maison in [13]. However this prescription like any others requires the introduction of evanescent counter terms before the reaction can be renormalized by the standard procedure. An example for the HVBM prescription is that the non-singlet axial vector operator gets renormalized in spite of the fact that it is conserved. This effect has to be undone by introducing an additional renormalization constant. This has also to be done for higher spin operators otherwise their anomalous dimensions do not equal the anomalous dimensions of the spin averaged operators. Also the Adler-Bardeen theorem [14] is violated which states that the Adler-Bell-Jackiw anomaly [15] does not receive higher order

QCD corrections. A scheme which is equivalent to HVBM is the one given by Akyeampong and Delbourgo [16]. Here the $\gamma_5$ matrix is replaced by the Levi-Civita tensor multiplied by four $\gamma$ matrices. If the Feynman and phase space integrals are calculated before the traces are taken the result is the same as in the complicated HVBM technique. More details are given in the next section.

Our paper is organized as follows. In Section 2 we introduce our notations and discuss the technicalities which are involved when using Akyeampong-Delbourgo prescription for the $\gamma_5$-matrix. In Section 3 we present the NNLO corrections to the coefficient functions of the polarized DY cross section $d\Delta\sigma/dQ$. In Section 4 we study the NNLO corrections to polarized DY production in proton-proton collisions at the RHIC. Notice that this study is not complete since the three-loop contributions to the splitting functions are not available yet so that the corresponding polarized parton densities are not known. The long formulae for the NNLO coefficient functions can be found in Appendix A.

## 2 Kinematics of the polarized Drell-Yan process and $\gamma_5$ scheme

The Drell-Yan process proceeds through the following reaction

$$H_1(P_1,S_1)+H_2(P_2,S_2)\to\gamma^*(q)+'X',\qquad \Big|\qquad \to l^+(l_1)+l^-(l_2)$$

$$S=(P_1+P_2)^2\,,\qquad Q^2\equiv q^2=(l_1+l_2)^2\,, \tag{2.1}$$

where $H_i$ $(i=1,2)$ represent the incoming polarized hadrons carrying the momenta $P_i$ and spins $S_i$. Further $'X'$ denotes any inclusive hadronic state which is unpolarized. The lepton pair is represented by $l^+l^-$ with momenta $l_1$, $l_2$. In this paper we will only consider lepton pairs which have a sufficiently small invariant mass $Q$ so that the photon dominates in the above reaction and $Z$-boson exchange effects can be neglected. The cross section is given by

$$\frac{d\,\Delta\,\sigma^{\mathrm{H_1H_2}}}{d\,Q^2}=\frac{4\pi\alpha^2}{3\,N\,Q^2\,S}\,\Delta W^{\mathrm{H_1H_2}}(\tau,Q^2)\,,\qquad \tau=\frac{Q^2}{S}\,. \tag{2.2}$$

In the QCD improved parton model the hadronic DY structure function $\Delta W^{\mathrm{H_1H_2}}$ is related to the coefficient functions $\Delta_{ij}$ as follows

$$\begin{aligned}\Delta W^{\mathrm{H_1H_2}}(\tau,Q^2) &= \sum_{i,j=q,\bar q,g}\int_\tau^1\frac{dx_1}{x_1}\int_{\tau/x_1}^1\frac{dx_2}{x_2}\,\Delta f_i^{\mathrm{H_1}}(x_1,\mu^2)\,\Delta f_j^{\mathrm{H_2}}(x_2,\mu^2)\\ &\times\Delta_{ij}\left(\frac{\tau}{x_1x_2},Q^2,\mu^2\right)\,.\end{aligned} \tag{2.3}$$

In the formula above $\Delta f_i(x,\mu^2)$ $(i=q,\bar q,g)$ are the polarized parton densities where $\mu$ denotes the factorization/renormalization scale and $x$ is the fraction of the hadron momentum carried by the parton. The DY partonic structure function $\Delta\hat W_{ij}$ is computed from the partonic subprocess

$$i(p_1,s_1)+j(p_2,s_2)\to\gamma^*(q)+i_1(k_1)\cdots i_n(k_n)\,, \tag{2.4}$$

and it reads

$$\Delta\hat W_{ij}=K_{ij}\int d^4q\,\delta(q^2-Q^2)$$

$$\times \prod_{i=1}^{n} \int \frac{d^3k_i}{(2\pi)^3\, 2E_i}\, \delta^{(4)}\left(p_1 + p_2 - q - \sum_{j=1}^{n} k_j\right)$$

$$\times |\Delta\hat{M}_{i+j\to\gamma^*+i_1\cdots i_n}|^2\,, \tag{2.5}$$

where $K_{ij}$ denotes the colour and spin average factors and the polarized matrix elements are denoted by $\Delta\hat{M}$ (when we refer to unpolarized structure functions, matrix elements and parton densities we drop the $\Delta$). Finally note that the relation between the parton densities above and the parton momentum densities appearing in the parton density sets in the literature or PDF libraries, which are denoted by $\Delta f_a^{\rm PDF}(x,\mu^2)$, is given by $\Delta f_a^{\rm PDF}(x,\mu^2) = x\ \Delta f_a(x,\mu^2)$.

When $|\Delta\hat{M}_{ij}|^2$ in Eq. (2.5) is calculated up to order $\alpha_s^2$ one encounters four partonic subprocesses which are characterised by the two partons in their initial state. In the case of quarks with a mass $m \neq 0$ they are given by

$$q(p_1,s_1) + \bar{q}(p_2,s_2) \to \gamma^* +' X'\,,$$

$$|\Delta\hat{M}_{q\bar{q}}|^2 = \frac{1}{4}\,\mathbf{Tr}\,\left(\gamma_5 \not{s}_2\,(\not{p}_2 - m)\,\tilde{M}\,\gamma_5 \not{s}_1\,(\not{p}_1 + m)\,\tilde{M}^\dagger\right)\,, \tag{2.6}$$

$$q_1(\bar{q}_1)(p_1,s_1) + g(p_2) \to \gamma^* +' X'\,,$$

$$|\Delta\hat{M}_{qg}|^2 = \frac{1}{4}\,\epsilon_{\mu\nu\lambda\sigma}\,\frac{p_2^\lambda\, l_2^\sigma}{p_2\cdot l_2}\,\mathbf{Tr}\,\left(\tilde{M}^\mu\,\gamma_5 \not{s}_1\,(\not{p}_1 \pm m)\,\tilde{M}^{\nu\dagger}\right)\,, \tag{2.7}$$

$$q_1(\bar{q}_1)(p_1,s_1) + q_2(\bar{q}_2)(p_2,s_2) \to \gamma^* +' X'$$

$$|\Delta\hat{M}_{q_1q_2}|^2 = \frac{1}{4}\,\mathbf{Tr}\,\left(\gamma_5 \not{s}_2\,(\not{p}_2 \pm m)\,\tilde{M}\,\gamma_5 \not{s}_1\,(\not{p}_1 \pm m)\,\tilde{M}^\dagger\right)\,, \tag{2.8}$$

$$g(p_1) + g(p_2) \to \gamma^* +' X'\,,$$

$$|\Delta\hat{M}_{gg}|^2 =$$

$$\frac{1}{4}\,\epsilon_{\mu_2\nu_2\lambda_2\sigma_2}\,\frac{p_2^{\lambda_2}\, l_2^{\sigma_2}}{p_2\cdot l_2}\,\epsilon_{\mu_1\nu_1\lambda_1\sigma_1}\,\frac{p_1^{\lambda_1}\, l_1^{\sigma_1}}{p_1\cdot l_1}\,\mathbf{Tr}\,\left(\tilde{M}^{\mu_1\mu_2}\,\tilde{M}^{\nu_1\nu_2\dagger}\right)\,, \tag{2.9}$$

where $\tilde{M}$ denotes the matrix element which is given by the standard Feynman rules. Further the symbol **Tr** can represent multiple traces when the matrix elements are calculated in higher order and for the reaction in Eq. (2.8) one must distinguish between $q_1 = q_2$ and $q_1 \neq q_2$. The spin vectors $s_i$ and the gauge vectors $l_i$ $(i = 1, 2)$ satisfy the properties

$$s_i \cdot p_i = 0\,, \qquad s_i \cdot s_i = -1\,, \qquad l_i \cdot l_i = 0\,. \tag{2.10}$$

When the (anti-)quark is massless then one has to make the replacements

$$\gamma_5 \not{s}_i \, (\not{p}_i \pm m) \to \pm \, \gamma_5 \, h_i \not{p}_i\,, \tag{2.11}$$

where $h_i$ $(i = 1, 2)$ represent the helicities of the incoming (anti-)quarks and the $+$ and $-$ signs on the right-hand side hold for the quarks and anti-quarks respectively. The definitions above are chosen in such a way that the partonic polarized structure function satisfies the property

$$\Delta W_{ij} = W_{ij}(+,+) - W_{ij}(+,-)\,, \tag{2.12}$$

with $+, -$ denoting the helicities of the incoming partons.

The computation of the matrix elements in Eqs. (2.6)-(2.9) and their virtual corrections reveals divergences which occur when the momenta over which one integrates tend to zero (infrared), infinity (ultraviolet) or collinear to another momentum (collinear). The most popular way to regularize these singularities is to choose the method of $n$-dimensional regularization [12] in which the space is extended to $n$ dimensions. The singularities are represented by pole terms of the type $(1/\varepsilon)^k$ with $n = 4 + \varepsilon$. This method is very useful because it preserves the Ward identities in the case of gauge theories. However this is no longer the case when the $\gamma_5$ matrix and the Levi-Civita tensor appear like in Eqs. (2.6)-(2.9) or in weak interactions. There is no consistent way to generalize these two quantities in $n$ dimensions contrary to the ordinary matrix $\gamma_\mu$ or the metric tensor $g_{\mu\nu}$. In the literature one has proposed various methods to extend the $\gamma_5$ matrix and the Levi-Civita tensor to $n$ dimensions but one always needs so-called evanescent counter terms [17] to restore the Ward identities. A very popular prescription is the HVBM-scheme which was proposed in [12] and generalized in [13]. In this approach the $n$-dimensional gamma-matrices and momenta have to be split into 4 and $n-4$ dimensional parts. Therefore also the integrals over the final

state momenta have to split up in the same way. Many NLO calculations have been done in this scheme (see e.g. [5]-[11]). However this approach requires a special procedure to deal with the gamma-matrix algebra which is not implemented in the program FORM [18]. Since this program is used in our calculations we prefer another prescription for the $\gamma_5$-matrix which is given in [16]. It gives the same results as the HVBM-scheme but it is much simpler to use in algebraic manipulation programs. Moreover one does not have to split up the integrals over the final state momenta and one can simply use the phase space integrals computed for unpolarized reactions. The procedure in [16] is given by

1. Replace the $\gamma_5$-matrix by

$$\gamma_\mu \, \gamma_5 = \frac{i}{6} \, \epsilon_{\mu\rho\sigma\tau} \, \gamma^\rho \, \gamma^\sigma \, \gamma^\tau \quad \text{or} \quad \gamma_5 = \frac{i}{24} \, \epsilon_{\rho\sigma\tau\kappa} \, \gamma^\rho \, \gamma^\sigma \, \gamma^\tau \, \gamma^\kappa \, .$$

2. Compute all matrix elements in $n$ dimensions.

3. Evaluate all Feynman integrals and phase space integrals in $n$-dimensions.

4. Contract the Levi-Civita tensors in four dimensions after the Feynman integrals and phase space integrals are carried out.

(2.13)

Note that the contraction in four dimensions only applies to Lorentz indices which are present in the Levi-Civita tensors. The last step in (2.13) requires that one first has to apply tensorial reduction to all integrals. For simple expressions this takes the form

$$\begin{aligned}
\int \frac{d^n \, k}{(2\pi)^n} \, k^\mu \, k^\nu \, f(k, p_1, p_2) &= A_{00}(n) \, g^{\mu\nu} + A_{11}(n) \, p_1^\mu \, p_1^\nu + A_{22}(n) \, p_2^\mu \, p_2^\nu \\
&\quad + A_{12}(n) \, p_1^\mu \, p_2^\nu + A_{21}(n) \, p_2^\mu \, p_1^\nu \, , \\
\int dPS^{(2)} \, k^\mu \, k^\nu \, f(k, p_1, p_2) &= B_{00}(n) \, g^{\mu\nu} + B_{11}(n) \, p_1^\mu \, p_1^\nu + B_{22}(n) \, p_2^\mu \, p_2^\nu \\
&\quad + B_{12}(n) \, p_1^\mu \, p_2^\nu + B_{21}(n) \, p_2^\mu \, p_1^\nu \, ,
\end{aligned}$$

(2.14)

where the coefficients $A_{ij}, B_{ij}$ depend on $n = 4 + \varepsilon$. However there exists an alternative method. If the matrix element only contains one $\gamma_5$ like in $qg$ or even none as in $gg$ one can apply a different rule. One replaces $\gamma_5$ according to 1 in Eq. (2.13) and one contracts the Levi-Civita tensors in $n$ dimensions before the Feynman integrals and phase space integrals are carried out. Further one factor of $1/2$ in Eqs. (2.7) and (2.9) is replaced by $1/(n-2)(n-3)$. The result is the same as given by the method in Eq. (2.13).

The HVBM-scheme or the prescription above automatically reproduces the Adler-Bell-Jackiw anomaly (ABJ) [15] but it violates the Ward identity for the non-singlet axial vector current and the Adler-Bardeen theorem [14]. In order to obtain the correct renormalized quantities one therefore needs to invoke additional counter terms [19], which are called evanescent [17] since they do not occur for $n = 4$. This procedure was used to obtain the NLO anomalous dimensions for the spin operators which determine the evolution of the parton spin densities see [20], [21]. Evanescent counter terms are also needed in cases where collinear divergences show up like in partonic cross sections (see e.g. [22]). This is characteristic for the HVBM scheme as well as any other approach. The reason is that in $n$-dimensional regularization there exists a one-to-one correspondence between the ultraviolet divergences occurring in partonic operator matrix elements and the collinear divergences appearing in partonic cross sections provided both quantities are of twist two type [22]. In [23] we have calculated all evanescent counter terms for the HVBM-scheme up to second order. For later convenience we will express them in the unrenormalized coupling constant

$$\begin{aligned} Z_{qq}^{5,\mathrm{NS},+} &= \delta(1-x) + \hat{a}_s\, S_\varepsilon \left(\frac{Q^2}{\mu^2}\right)^{\varepsilon/2} \left[ z_{qq}^{(1)} + \varepsilon \bar{z}_{qq}^{(1)} \right] + \hat{a}_s^2\, S_\varepsilon^2 \left(\frac{Q^2}{\mu^2}\right)^{\varepsilon} \Bigg[ \\ &\quad -\frac{1}{\varepsilon}\,\beta_0\, z_{qq}^{(1)} + z_{qq}^{(2),\mathrm{NS},+} - 2\,\beta_0\, \bar{z}_{qq}^{(1)} \Bigg], \\ a_s &= \frac{\alpha_s(\mu^2)}{4\pi}, \end{aligned} \tag{2.15}$$

$$Z_{qq}^{5,\mathrm{NS},-} = -\hat{a}_s^2\, S_\varepsilon^2 \left(\frac{Q^2}{\mu^2}\right)^{\varepsilon} \left[ z_{qq}^{(2),\mathrm{NS},-} \right], \tag{2.16}$$

$$Z_{qq}^{5,\rm PS} = \hat{a}_s^2\, S_\varepsilon^2\, \left(\frac{Q^2}{\mu^2}\right)^{\varepsilon}\, \left[z_{qq}^{(2),\rm PS}\right], \tag{2.17}$$

where $\beta_0$ represents the lowest order coefficient in the beta-function. Note that we have to take $\ln Q^2/\mu^2$ terms into account otherwise it is impossible to relate $\Delta\hat{W}_{q\bar{q}}^{\rm NS}$ to the unpolarized expression $\hat{W}_{q\bar{q}}^{\rm NS}$. This follows from the definition of $Z_{qq}^{5,\rm NS,+}$

$$\left(Z_{qq}^{5,\rm NS,+}\right)^2 = -\frac{\Delta\hat{W}_{q\bar{q}}^{\rm NS}(\hat{a}_s, Q^2/\mu^2)}{\hat{W}_{q\bar{q}}^{\rm NS}(\hat{a}_s, Q^2/\mu^2)} \tag{2.18}$$

Explicitly we can write

$$\begin{aligned}
Z_{qq}^{5,\rm NS,+}(x) &= \delta(1-x) + \hat{a}_s\, S_\varepsilon\, \left(\frac{Q^2}{\mu^2}\right)^{\varepsilon/2}\, C_F \Bigg[ -8(1-x) + \varepsilon\Big\{ \\
&\quad -8(1-x)\ln(1-x) + 4(1-x)\ln x + 4 - 4x\Big\}\Bigg] \\
&\quad +\hat{a}_s^2\, S_\varepsilon^2\, \left(\frac{Q^2}{\mu^2}\right)^{\varepsilon}\, \Bigg[C_F^2\Big\{ -16(1-x) - (16+8x)\ln x \\
&\quad +16(1-x)\ln x \ln(1-x)\Big\} \\
&\quad +C_A C_F\Big\{\frac{1}{\varepsilon}\Big(\frac{88}{3}(1-x)\Big) - \frac{856}{9}(1-x) + 8(1-x)\zeta(2) \\
&\quad +\frac{176}{3}\,(1-x)\,\ln(1-x) + (-\frac{168}{3} + 32\,x)\ln x - 4(1-x)\ln^2 x\Big\} \\
&\quad +n_f C_F T_f\Big\{ -\frac{1}{\varepsilon}\Big(\frac{32}{3}(1-x)\Big) + \frac{176}{9}(1-x) + 16\,(1-x)\ln x \\
&\quad -\frac{64}{3}\,(1-x)\,\ln(1-x)\Big\}\Bigg], \qquad (2.19)
\end{aligned}$$

$$Z_{qq}^{5,\rm NS,-} = -\hat{a}_s^2\, S_\varepsilon^2\, \left(\frac{Q^2}{\mu^2}\right)^{\varepsilon}\, \Big(C_F^2 - \frac{1}{2}C_A C_F\Big)\, \Big[8(1+x)\Big(4{\rm Li}_2(-x)$$

$$+4\ln x\ln(1+x)+2\zeta(2)-\ln^2 x-3\ln x\Big)-56(1-x)\Bigg]\,, \tag{2.20}$$

$$Z_{qq}^{5,\mathrm{PS}} \;=\; \hat{a}_s^2\,S_\varepsilon^2\left(\frac{Q^2}{\mu^2}\right)^{\varepsilon} n_f\,C_F\,T_f\left[16(1-x)+8(3-x)\ln x+4(2+x)\ln^2 x\right]. \tag{2.21}$$

A comparison with previous calculations [22], [23] shows that the evanescent counter terms are universal except for the $Q^2/\mu^2$ terms and the $\varepsilon$ part of the order $\hat{a}_s$ contribution.

# 3 Corrections up to NNLO to polarized Drell-Yan production

In this section we treat the various subprocesses which contribute to the Drell-Yan reaction up to NNLO. The Born reaction is given by the process

$$q + \bar{q} \to \gamma^* \,. \tag{3.1}$$

The first order corrections are given by the following subprocesses. The bremsstrahlung reaction to the Born process

$$q + \bar{q} \to \gamma^* + g \,, \tag{3.2}$$

plus the one-loop correction to the Born process. Further we have a new process with a gluon in the initial state

$$g + q(\bar{q}) \to \gamma^* + q(\bar{q}) \,. \tag{3.3}$$

In the next order we encounter the following processes. First we have the bremsstrahlung correction to reaction (3.2)

$$q + \bar{q} \to \gamma^* + g + g \,, \tag{3.4}$$

plus the two-loop correction to the Born process and the one-loop corrections to process (3.2). Next we have the bremsstrahlung correction to reaction (3.3)

$$g + q(\bar{q}) \to \gamma^* + q(\bar{q}) + g \,, \tag{3.5}$$

plus the one-loop correction to reaction (3.3). Subsequently we have three new reactions. The first involves a quark-anti-quark reaction see Figs. 1, 2

$$q + \bar{q} \to \gamma^* + q + \bar{q} \,, \tag{3.6}$$

and the second contains two (anti-) quarks in the initial state see Figs. 2, 3

$$q(\bar{q}) + q(\bar{q}) \to \gamma^* + q(\bar{q}) + q(\bar{q}) \,, \tag{3.7}$$

In the above reaction the quarks can be equal or unequal. Finally we have a reaction with two gluons in the initial state

$$g + g \to \gamma^* + q + \bar{q} \,. \tag{3.8}$$

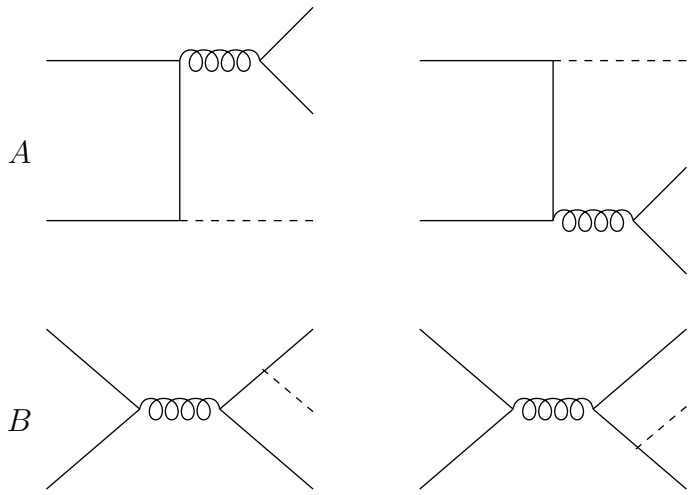



Figure 1: Annihilation graphs contributing to the subprocess $q + \bar{q} \to \gamma^* + q + \bar{q}$.

All matrix elements are calculated in $n$-dimensions using the algebraic manipulation program FORM [18]. The phase space integration and the Feynman integration are explained in [24] and [25]. The results can be expressed in the renormalization group coefficients $\Delta P_{ij}$, $\beta_0$ and $w_{kl}^{(i)}$ as follows

$$
\begin{aligned}
-\Delta\hat{W}_{q\bar{q}}^{\rm NS} &= \delta(1-z) + \hat{a}_s\, S_\varepsilon \left(\frac{Q^2}{\mu^2}\right)^{\varepsilon/2} \left[\frac{2}{\varepsilon}\,\Delta P_{qq}^{(0)} + w_{q\bar{q}}^{(1)} + 2\, z_{qq}^{(1)} + \right. \\
&\left. +\varepsilon\, \left(\bar{w}_{q\bar{q}}^{(1)} + 2\,\bar{z}_{qq}^{(1)}\right)\right] + \hat{a}_s^2\, S_\varepsilon^2 \left(\frac{Q^2}{\mu^2}\right)^{\varepsilon} \left[\frac{1}{\varepsilon^2}\left\{2\,\Delta P_{qq}^{(0)} \otimes \Delta P_{qq}^{(0)} \right.\right. \\
&\left. -2\,\beta_0\,\Delta P_{qq}^{(0)}\right\} + \frac{1}{\varepsilon}\left\{\Delta P_{qq}^{(1),{\rm NS},+} + 2\,\Delta P_{qq}^{(0)} \otimes w_{q\bar{q}}^{(1)} - 2\,\beta_0\, w_{q\bar{q}}^{(1)} \right. \\
&\left. +4\, z_{qq}^{(1)} \otimes \Delta P_{qq}^{(0)} - 2\,\beta_0\, z_{qq}^{(1)}\right\} + 2\,\Delta P_{qq}^{(0)} \otimes \bar{w}_{q\bar{q}}^{(1)} - 2\,\beta_0\,\bar{w}_{q\bar{q}}^{(1)} \\
&+ w_{q\bar{q}}^{(2),{\rm NS}} + 4\,\bar{z}_{qq}^{(1)} \otimes \Delta P_{qq}^{(0)} + 2\, z_{qq}^{(1)} \otimes w_{q\bar{q}}^{(1)} + z_{qq}^{(1)} \otimes z_{qq}^{(1)}
\end{aligned}
$$

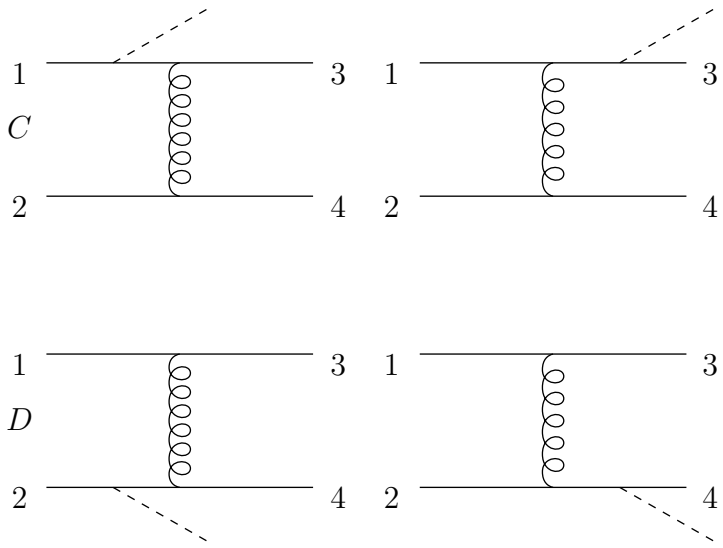



Figure 2: Gluon exchange graphs contributing to the subprocess $q + \bar{q} \to \gamma^* + q + \bar{q}$ and $q + q \to \gamma^* + q + q$.

$$-4\,\beta_0\,\bar{z}_{qq}^{(1)} + 2\,z_{qq}^{(2),\mathrm{NS},+}\Bigg], \tag{3.9}$$

$$\begin{aligned}
\Delta\hat{W}_{qg} \;=\; & -\hat{a}_s\,S_\varepsilon\left(\frac{Q^2}{\mu^2}\right)^{\varepsilon/2}\left[\frac{1}{2\varepsilon}\,\Delta P_{qg}^{(0)} + w_{qg}^{(1)} + \varepsilon\,\bar{w}_{qg}^{(1)}\right] - \hat{a}_s^2\,S_\varepsilon^2\left(\frac{Q^2}{\mu^2}\right)^{\varepsilon} \\
& \times\Bigg[\frac{1}{\varepsilon^2}\left\{\frac{3}{4}\,\Delta P_{qq}^{(0)}\otimes\Delta P_{qg}^{(0)} + \frac{1}{4}\,\Delta P_{gg}^{(0)}\otimes\Delta P_{qg}^{(0)} - \frac{1}{2}\,\beta_0\,\Delta P_{qg}^{(0)}\right\} \\
& + \frac{1}{\varepsilon}\left\{\frac{1}{4}\,\Delta P_{qg}^{(1)} - 2\,\beta_0\,w_{qg}^{(1)} + \frac{1}{2}\,\Delta P_{qg}^{(0)}\otimes w_{q\bar{q}}^{(1)} + \left(\Delta P_{qq}^{(0)} + \Delta P_{gg}^{(0)}\right)\right. \\
& \left.\otimes w_{qg}^{(1)} + \frac{3}{4}\,z_{qq}^{(1)}\otimes\Delta P_{qg}^{(0)}\right\} - 2\,\beta_0\,\bar{w}_{qg}^{(1)} + \frac{1}{2}\,\Delta P_{qg}^{(0)}\otimes\bar{w}_{q\bar{q}}^{(1)} + \Big(\Delta P_{qq}^{(0)} \\
& + \Delta P_{gg}^{(0)}\Big)\otimes\bar{w}_{qg}^{(1)} + w_{qg}^{(2)} + \frac{1}{2}\,\bar{z}_{qq}^{(1)}\otimes\Delta P_{qg}^{(0)} + z_{qq}^{(1)}\otimes w_{qg}^{(1)}\Bigg].
\end{aligned} \tag{3.10}$$

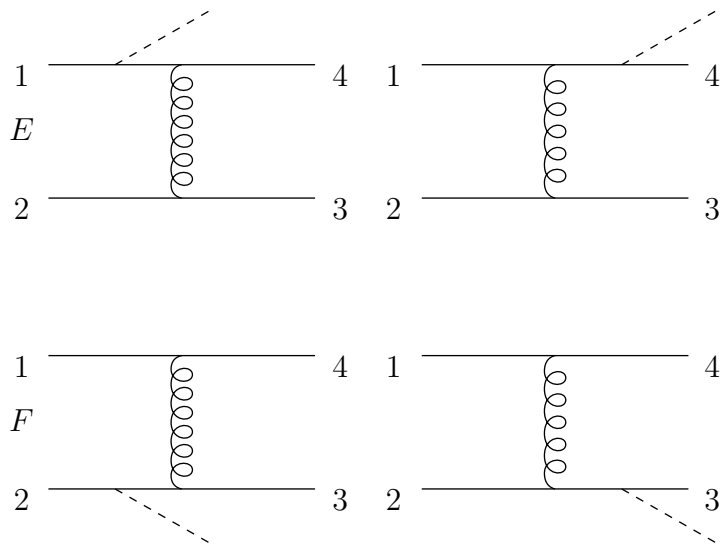



Figure 3: Gluon exchange graphs contributing to the subprocess $q + q \to \gamma^* + q + q$ with identical quarks in the initial and/or final state.

The $q\bar{q}$ reaction (see Figs. 1,2) yields

$$\Delta\hat{W}_{q\bar{q}}^{\rm PS} = -\hat{a}_s^2\, S_\varepsilon^2 \left(\frac{Q^2}{\mu^2}\right)^\varepsilon \left[\frac{1}{2\varepsilon^2}\,\Delta P_{qg}^{(0)} \otimes \Delta P_{gq}^{(0)} + \frac{1}{\varepsilon}\left\{\frac{1}{2}\,\Delta P_{qq}^{(1),{\rm PS}} + 2\,\Delta P_{gq}^{(0)} \otimes w_{qg}^{(0)}\right\} + 2\,\Delta P_{gq}^{(0)} \otimes \bar{w}_{qg}^{(1)} + w_{q\bar{q}}^{(2),{\rm PS}} + 2\, z_{qq}^{(2),{\rm PS}}\right]. \tag{3.11}$$

The $q\bar{q}$ can be split into $q_1\bar{q}_2$ ($q_1 \neq q_2$) and a $q\bar{q}$ reaction. The latter does include Fig. 1B.

$$w_{q_1\bar{q}_2}^{(2),{\rm PS}} = w_{CC}^{(2)} + w_{DD}^{(2)} + w_{CD}^{(2)}\,, \tag{3.12}$$

$$w_{q\bar{q}}^{(2),{\rm PS}} = w_{BB}^{(2)} + w_{BC}^{(2)} + w_{BD}^{(2)} + w_{CC}^{(2)} + w_{DD}^{(2)} + w_{CD}^{(2)}\,. \tag{3.13}$$

Processes with unequal quarks in the final state (see Fig. 2) yields

$$\Delta\hat{W}_{q_1q_2} = -\hat{a}_s^2\, S_\varepsilon^2 \left(\frac{Q^2}{\mu^2}\right)^\varepsilon \left[\frac{1}{2\varepsilon^2}\,\Delta P_{qg}^{(0)} \otimes \Delta P_{gq}^{(0)} + \frac{1}{\varepsilon}\left\{\frac{1}{2}\,\Delta P_{qq}^{(1),\mathrm{PS}} + 2\,\Delta P_{gq}^{(0)} \otimes w_{qg}^{(0)}\right\} + 2\,\Delta P_{gq}^{(0)} \otimes \bar{w}_{qg}^{(1)} + w_{q_1q_2}^{(2)} + 2\, z_{qq}^{(2),\mathrm{PS}}\right] \quad (3.14)$$

$$w_{q_1q_2}^{(2)} = w_{CC}^{(2)} + w_{DD}^{(2)} + w_{CD}^{(2)}\,. \quad (3.15)$$

Processes with equal quarks in the final state (see Figs. 2, 3) yields

$$\Delta\hat{W}_{qq} = -\hat{a}_s^2\, S_\varepsilon^2 \left(\frac{Q^2}{\mu^2}\right)^\varepsilon \left[\frac{1}{2\varepsilon^2}\,\Delta P_{qg}^{(0)} \otimes \Delta P_{gq}^{(0)} + \frac{1}{\varepsilon}\left\{\frac{1}{2}\,\Delta P_{qq}^{(1),\mathrm{PS}} - \Delta P_{qq}^{(1),\mathrm{NS},-} + 2\,\Delta P_{gq}^{(0)} \otimes w_{qg}^{(0)}\right\} + 2\,\Delta P_{gq}^{(0)} \otimes \bar{w}_{qg}^{(1)} + w_{qq}^{(2)} + 2\, z_{qq}^{(2),\mathrm{PS}} - 2\, z_{qq}^{(2),\mathrm{NS},-}\right], \quad (3.16)$$

$$w_{qq}^{(2)} = w_{CC}^{(2)} + w_{DD}^{(2)} + w_{CD}^{(2)} + w_{FF}^{(2)} + w_{EE}^{(2)} + w_{FE}^{(2)} + w_{CF}^{(2)} + w_{CE}^{(2)} + w_{DF}^{(2)} + w_{DE}^{(2)}\,. \quad (3.17)$$

Finally we have the gluon-gluon scattering process

$$\Delta\hat{W}_{gg} = -\hat{a}_s^2\, S_\varepsilon^2 \left(\frac{Q^2}{\mu^2}\right)^\varepsilon \left[\frac{1}{2\varepsilon^2}\,\Delta P_{qg}^{(0)} \otimes \Delta P_{qg}^{(0)} + \frac{2}{\varepsilon}\,\Delta P_{qg}^{(0)} \otimes w_{qg}^{(1)} + 2\,\Delta P_{qg}^{(0)} \otimes \bar{w}_{qg}^{(1)} + w_{gg}^{(2)}\right], \quad (3.18)$$

where $\otimes$ denotes the convolution symbol defined by

$$f \otimes g(z) = \int_0^1 dz_1 \int_0^1 dz_2\, \delta(z - z_1\, z_2)\, f(z_1)\, g(z_2)\,. \quad (3.19)$$

The expressions follow from the renormalization group equations. They are constructed in such a way that they become finite after coupling constant renormalization and mass factorization are carried out. The $\beta_0$ appears as the lowest order coefficient in the beta-function. The splitting function $\Delta P_{ij}(z)$ and the coefficients $w_{ij}^{(i)}(z)$ with $z = Q^2/s$ also occur in the coefficient functions given below except for the NLO terms $\bar{w}_{ij}^{(1)}$, which are proportional to $\varepsilon$. They are given by

$$\begin{aligned}
\bar{w}_{q\bar{q}}^{(1)} &= C_F \left[ 8\,\mathcal{D}_2(x) - 6\,\zeta(2)\,\mathcal{D}_0(x) + (1+x)\left( -4\,\ln^2(1-x) + 3\,\zeta(2)\right)\right. \\
&\quad + \frac{1+x^2}{1-x}\left(-4\,\ln x\,\ln(1-x) + \ln^2 x\right) + 4\,(1-x) + \delta(1-x)\left(16\right. \\
&\quad \left.\left. - \frac{21}{2}\,\zeta(2)\right)\right], \qquad (3.20)
\end{aligned}$$

$$\begin{aligned}
\bar{w}_{qg}^{(1)} &= T_f \left[ \frac{1}{2}\,(2\,x-1)\left(\ln^2\left(\frac{(1-x)^2}{x}\right) - 3\,\zeta(2)\right) + \left(\frac{5}{2} - x - \frac{3}{2}\,x^2\right)\right. \\
&\quad \left. \times \ln\left(\frac{(1-x)^2}{x}\right) - 5 + 4\,x + x^2\right], \qquad (3.21)
\end{aligned}$$

where $\mathcal{D}_i$ denotes the distribution

$$\mathcal{D}_i = \left(\frac{\ln^i(1-z)}{1-z}\right)_+ . \qquad (3.22)$$

To render the partonic cross sections finite one has first to perform coupling constant renormalization. This is done by replacing the bare coupling constant by the renormalized one i.e.

$$\hat{a}_s = a_s(\mu^2)\left[1 + a_s(\mu^2)\,S_\varepsilon\,\frac{2}{\varepsilon}\,\beta_0 + \cdots\right]. \qquad (3.23)$$

To remove the evanescent counter terms we perform the following operation. We multiply each quark line with the inverse of $Z_{qq}^5$ [22]. This means that

$q\bar{q}$, $qq$ and $q_1q_2$ are multiplied by $(Z_{qq}^5)^{-2}$. The $qg$ is multiplied by $(Z_{qq}^5)^{-1}$ and the $gg$ subprocess gets no factor. The remaining divergences, which are of collinear origin, are removed by mass factorization

$$\left(Z_{qq}^5\right)^{-\alpha} \Delta\hat{W}_{ij}\left(\frac{1}{\varepsilon},\frac{Q^2}{\mu^2}\right) = \sum_{k,l=q,\bar{q},g} \Gamma_{ki}\left(\frac{1}{\varepsilon}\right) \otimes \Gamma_{lj}\left(\frac{1}{\varepsilon}\right) \otimes \Delta_{kl}\left(\frac{Q^2}{\mu^2}\right) , \quad (3.24)$$

where $\alpha$ is the number of (anti)-quarks in the initial state. Further $\Gamma_{ki}(z)$ denote the kernels containing the splitting function which multiply the collinear divergences represented by the pole terms $1/\varepsilon^k$. For the different subprocesses the mass factorization relations in Eq.(3.24) become equal to

$$\left(Z_{qq}^5\right)^{-2} \Delta\hat{W}_{q\bar{q}}^{\rm NS} = \Gamma_{qq}^{\rm NS} \otimes \Gamma_{\bar{q}\bar{q}}^{\rm NS} \otimes \Delta_{q\bar{q}}^{\rm NS} , \quad (3.25)$$

$$\left(Z_{qq}^5\right)^{-1} \Delta\hat{W}_{qg} = \Gamma_{qq} \otimes \Gamma_{\bar{q}g} \otimes \Delta_{q\bar{q}} + \Gamma_{qq} \otimes \Gamma_{gg} \otimes \Delta_{qg} , \quad (3.26)$$

$$\left(Z_{qq}^5\right)^{-2} \Delta\hat{W}_{q\bar{q}} = \Gamma_{qq} \otimes \Gamma_{\bar{q}\bar{q}} \otimes \Delta_{q\bar{q}} + \Gamma_{g\bar{q}} \otimes \Gamma_{qq} \otimes \Delta_{gq} + \Gamma_{gq} \otimes \Gamma_{\bar{q}\bar{q}} \otimes \Delta_{g\bar{q}} , \quad (3.27)$$

$$\begin{aligned}\left(Z_{qq}^5\right)^{-2} \Delta\hat{W}_{q_1q_2} &= \Gamma_{q_1q_1} \otimes \Gamma_{q_1q_2} \otimes \Delta_{qq} + \Gamma_{gq_1} \otimes \Gamma_{q_2q_2} \otimes \Delta_{gq_2} \\ &\quad + \Gamma_{gq_2} \otimes \Gamma_{q_1q_1} \otimes \Delta_{gq_1} , \end{aligned} \quad (3.28)$$

$$\begin{aligned}\left(Z_{qq}^5\right)^{-2} \Delta\hat{W}_{qq} &= \Gamma_{qq} \otimes \Gamma_{\bar{q}q} \otimes \Delta_{q\bar{q}} + \Gamma_{\bar{q}q} \otimes \Gamma_{qq} \otimes \Delta_{\bar{q}q} + \Gamma_{gq} \otimes \Gamma_{qq} \otimes \Delta_{gq} \\ &\quad + \Gamma_{qq} \otimes \Gamma_{gq} \otimes \Delta_{qg} + \Gamma_{qq} \otimes \Gamma_{qq} \otimes \Delta_{qq} , \end{aligned} \quad (3.29)$$

$$\begin{aligned}\Delta\hat{W}_{gg} &= 2\,\Gamma_{qg} \otimes \Gamma_{\bar{q}g} \otimes \Delta_{q\bar{q}} + 2\,\Gamma_{\bar{q}g} \otimes \Gamma_{gg} \otimes \Delta_{qg} + 2\,\Gamma_{\bar{q}g} \otimes \Gamma_{gg} \otimes \Delta_{\bar{q}g} \\ &\quad + \Gamma_{gg} \otimes \Gamma_{gg} \otimes \Delta_{gg} . \end{aligned} \quad (3.30)$$

Since we need the finite expressions up to order $\alpha_s^2$ it is sufficient to expand the kernels $\Gamma_{ki}$ up to the following order in the renormalized coupling constant

$$\begin{aligned}\Gamma_{qq}^{\rm NS} &= \Gamma_{\bar{q}\bar{q}}^{\rm NS} = \delta(1-z) + \hat{a}_s\, S_\varepsilon \left[\frac{1}{\varepsilon}\,\Delta P_{qq}^{(0)}\right] + \hat{a}_s^2\, S_\varepsilon^2 \left[\frac{1}{2\varepsilon^2}\Big(\Delta P_{qq}^{(0)} \otimes \Delta P_{qq}^{(0)} \right. \\ &\quad \left. - 2\,\beta_0\,\Delta P_{qq}^{(0)}\Big) + \frac{1}{2\varepsilon}\,\Delta P_{qq}^{(1),{\rm NS},+}\right] , \end{aligned} \quad (3.31)$$

$$\Gamma_{qg} = \Gamma_{\bar{q}g} = \hat{a}_s\, S_\varepsilon \left[\frac{1}{2\varepsilon}\,\Delta P_{qg}^{(0)}\right] + \hat{a}_s^2\, S_\varepsilon^2 \left[\frac{1}{4\varepsilon^2}\Big(\Delta P_{qg}^{(0)} \otimes \Delta P_{gg}^{(0)} + \Delta P_{qq}^{(0)} \otimes \Delta P_{qg}^{(0)} - 2\,\beta_0\,\Delta P_{qg}^{(0)}\Big) + \frac{1}{4\varepsilon}\Big(\Delta P_{qg}^{(1)} + \Delta P_{qg}^{(0)} \otimes z_{qq}^{(1)}\Big)\right], \tag{3.32}$$

$$\Gamma_{qq}^{\rm PS} = \Gamma_{\bar{q}\bar{q}}^{\rm PS} = \Gamma_{q\bar{q}}^{\rm PS} = \Gamma_{\bar{q}q}^{\rm PS} = \hat{a}_s^2\, S_\varepsilon^2 \left[\frac{1}{4\varepsilon^2}\,\Delta P_{qg}^{(0)} \otimes \Delta P_{gq}^{(0)} + \frac{1}{4\varepsilon}\,\Delta P_{qq}^{(1),{\rm PS}}\right], \tag{3.33}$$

$$\Gamma_{q\bar{q}}^{\rm NS} = \Gamma_{\bar{q}q}^{\rm NS} = -\hat{a}_s^2\, S_\varepsilon^2 \left[\frac{1}{2\varepsilon}\,\Delta P_{qq}^{(1),{\rm NS},-}\right], \tag{3.34}$$

$$\Gamma_{gq} = \Gamma_{g\bar{q}} = \hat{a}_s\, S_\varepsilon \left[\frac{1}{\varepsilon}\,\Delta P_{gq}^{(0)}\right], \tag{3.35}$$

$$\Gamma_{gg} = \delta(1-z) + \hat{a}_s\, S_\varepsilon \left[\frac{1}{\varepsilon}\,\Delta P_{gg}^{(0)}\right]. \tag{3.36}$$

After renormalization and mass factorization the coefficient functions have the following algebraic form

$$\Delta_{q\bar{q}}^{\rm NS} = -\delta(1-z) - a_s(\mu^2)\left[\Delta P_{qq}^{(0)}\,\ln\frac{Q^2}{\mu^2} + w_{q\bar{q}}^{(1)}\right] - a_s^2(\mu^2)\Bigg[\Big\{\frac{1}{2}\,\Delta P_{qq}^{(0)} \otimes \Delta P_{qq}^{(0)} - \frac{1}{2}\,\beta_0\,\Delta P_{qq}^{(0)}\Big\}\,\ln^2\frac{Q^2}{\mu^2} + \Big\{\Delta P^{(1),{\rm NS},+} - \beta_0\, w_{q\bar{q}}^{(1)} + \Delta P_{qq}^{(0)} \otimes w_{q\bar{q}}^{(1)}\Big\}\ln\frac{Q^2}{\mu^2} + w_{q\bar{q}}^{(2),{\rm NS}}\Bigg], \tag{3.37}$$

$$\Delta_{qg} = -a_s(\mu^2)\left[\frac{1}{4}\,\Delta P_{qg}^{(0)}\,\ln\frac{Q^2}{\mu^2} + w_{qg}^{(1)}\right] - a_s^2(\mu^2)\left[\Big\{\frac{1}{16}\,\Delta P_{qg}^{(0)} \otimes \Big(3\,\Delta P_{qq}^{(0)}\right.$$

$$+\Delta P_{gg}^{(0)}\Big) - \frac{1}{8}\,\beta_0\,\Delta P_{qg}^{(0)}\Big\}\,\ln^2\frac{Q^2}{\mu^2} + \Big\{\frac{1}{4}\Delta P_{qg}^{(1)} - \beta_0\,w_{qg}^{(1)} + \frac{1}{2}\,w_{qg}^{(1)}$$

$$\otimes\Big(\Delta P_{qq}^{(0)} + \Delta P_{gg}^{(0)}\Big) + \frac{1}{4}\,\Delta P_{qg}^{(0)} \otimes w_{q\bar{q}}^{(1)} + \frac{1}{4}\,\Delta P_{qg}^{(0)} \otimes z_{qq}^{(1)}\Big\}\,\ln\frac{Q^2}{\mu^2}$$

$$+w_{qg}^{(2)}\Bigg], \tag{3.38}$$

$$\Delta_{q\bar{q}}^{\rm PS} = -a_s^2(\mu^2)\,\Bigg[\Big\{\frac{1}{8}\Delta P_{qg}^{(0)} \otimes \Delta P_{gq}^{(0)}\Big\}\,\ln^2\frac{Q^2}{\mu^2} + \Big\{\frac{1}{2}\,\Delta P_{qq}^{(1),\rm PS}$$

$$+\Delta P_{gq}^{(0)} \otimes w_{qg}^{(1)}\Big\}\ln\frac{Q^2}{\mu^2} + w_{q\bar{q}}^{(2),\rm PS}\Bigg], \tag{3.39}$$

$$\Delta_{q_1q_2} = -a_s^2(\mu^2)\,\Bigg[\Big\{\frac{1}{8}\Delta P_{qg}^{(0)} \otimes \Delta P_{gq}^{(0)}\Big\}\,\ln^2\frac{Q^2}{\mu^2} + \Big\{\frac{1}{2}\,\Delta P_{qq}^{(1),\rm PS}$$

$$+\Delta P_{gq}^{(0)} \otimes w_{qg}^{(1)}\Big\}\ln\frac{Q^2}{\mu^2} + w_{q_1q_2}^{(2)}\Bigg], \tag{3.40}$$

$$\Delta_{qq} = -a_s^2(\mu^2)\,\Bigg[\Big\{\frac{1}{8}\Delta P_{qg}^{(0)} \otimes \Delta P_{gq}^{(0)}\Big\}\,\ln^2\frac{Q^2}{\mu^2} + \Big\{\frac{1}{2}\,\Delta P_{qq}^{(1),\rm PS} - \Delta P_{q\bar{q}}^{(1),\rm NS,-}$$

$$+\Delta P_{gq}^{(0)} \otimes w_{qg}^{(1)}\Big\}\ln\frac{Q^2}{\mu^2} + w_{qq}^{(2)}\Bigg], \tag{3.41}$$

$$\Delta_{gg} = -a_s^2(\mu^2)\,\Bigg[\Big\{\frac{1}{8}\,\Delta P_{qg}^{(0)} \otimes \Delta P_{qg}^{(0)}\Big\}\,\ln^2\frac{Q^2}{\mu^2} + \Big\{\Delta P_{qg}^{(0)} \otimes w_{qg}^{(1)}\Big\}\,\ln\frac{Q^2}{\mu^2}$$

$$+w_{gg}^{(2)}\Bigg]. \tag{3.42}$$

In Appendix A we give the explicit expressions for the coefficient functions so that one can determine the coefficients $\Delta P_{ij}^{(k)}$ and $w_{ij}^{(k)}$. One of the features

is that the non-singlet part of the structure function satisfies the relation

$$\left(Z_{qq}^{5,\mathrm{NS},+}\right)^{-2}\,\Delta\hat{W}_{q\bar{q}}^{\mathrm{NS}} = -\hat{W}_{q\bar{q}}^{\mathrm{NS}}\,. \tag{3.43}$$

For the $\mathrm{O}(\alpha_s^2)$ correction this holds for Eqs. (A.1)-(A.13). In the presentation of the coefficient functions above we have put the renormalization scale $\mu_r$ equal to the mass factorization scale $\mu$. If one wants to distinguish between both scales one can make the simple substitution

$$\alpha_s(\mu^2) = \alpha_s(\mu_r^2)\left[1 + \frac{\alpha_s(\mu_r^2)}{4\pi}\,\beta_0\,\ln\frac{\mu_r^2}{\mu^2}\right]. \tag{3.44}$$

# 4 $d\Delta\sigma/dQ$ for the process $p + p \to \gamma^* +' X'$

In this section we will present total cross sections (see Eq. (2.2)) for polarized Drell-Yan production in proton-proton collisions at the RHIC and make a comparison with similar results in previous work. The cross section can be rewritten as

$$\frac{d\Delta\sigma}{dQ} = \frac{8\,\pi\,\alpha^2}{3\,N\,S\,Q} \sum_{i,j=q,\bar{q},g} \int_\tau^1 \frac{dy}{y}\,\Phi_{ij}(y,\mu^2)\,\Delta_{ij}\left(\frac{\tau}{y},\frac{Q^2}{\mu^2}\right)\,, \tag{4.1}$$

where $\tau = Q^2/S$ and $\Phi_{ij}$ is the parton-parton flux defined by

$$\Phi_{ij}(y,\mu^2) = \int_y^1 \frac{du}{u}\,\Delta f_i(u,\mu^2)\,\Delta f_j\left(\frac{y}{u},\mu^2\right)\,. \tag{4.2}$$

In particular we study the dependence of the cross section on the input parameters such as the renormalization/factorization scale $\mu$, the virtuality of the photon $Q$ and the input parton densities. At this moment LO and NLO polarized parton densities are available but NNLO are not. Therefore an exact NNLO polarized cross section cannot be determined yet. Even an approximated polarized cross section cannot be given because a finite moment analysis of the anomalous dimensions is not yet available. Only the non-singlet anomalous dimension is known at least up to $N = 14$ [26]. Because of a lack of data the polarized parton density sets show a larger variation than in the unpolarized density sets. This in particular holds for the sea-quark and the gluon densities. For this reason polarized Drell-Yan production is very useful. The sea-quark contribution is dominant for the totally integrated cross section in proton-proton collisions while the gluon contribution dominates the differential distribution w.r.t. $p_T$ for $p_T > Q/2$. We shall use BB set 1 (BB1) for our plots [27] in the whole paper except for the longitudinal asymmetry where we shall choose also other density sets like BB set 2 (BB2) [27], the GRSV01 (standard scenario) and GRSV01 (valence scenario) [28]. The gluon in BB1 is larger than in BB2. In its turn the gluon in the standard scenario is smaller than in BB2 but larger than in the valence scenario. For all these sets LO and NLO versions exist. It is clear that in the case of LO we will use the one-loop parametrization for the running coupling constant and for NLO the two-loop corrected running coupling constant. However for an estimate of the NNLO corrections we

| | | |
|---|---|---|
| GRSV01 (LO, standard scenario) | $\Lambda_4^{\rm LO} = 175$ MeV | $\alpha_s^{\rm LO}(M_Z) = 0.121$ |
| GRSV01 (NLO, standard scenario) | $\Lambda_4^{\rm NLO} = 257$ MeV | $\alpha_s^{\rm NLO}(M_Z) = 0.109$ |
| GRSV01 (LO, valence scenario) | $\Lambda_4^{\rm LO} = 175$ MeV | $\alpha_s^{\rm LO}(M_Z) = 0.121$ |
| GRSV01 (NLO, valence scenario) | $\Lambda_4^{\rm NLO} = 257$ MeV | $\alpha_s^{\rm NLO}(M_Z) = 0.109$ |
| BB (LO, scenario 1) | $\Lambda_4^{\rm LO} = 203$ MeV | $\alpha_s^{\rm LO}(M_Z) = 0.123$ |
| BB (NLO, scenario 1) | $\Lambda_4^{\rm NLO} = 235$ MeV | $\alpha_s^{\rm NLO}(M_Z) = 0.107$ |
| BB (LO, scenario 2) | $\Lambda_4^{\rm LO} = 195$ MeV | $\alpha_s^{\rm LO}(M_Z) = 0.123$ |
| BB (NLO, scenario 2) | $\Lambda_4^{\rm NLO} = 240$ MeV | $\alpha_s^{\rm NLO}(M_Z) = 0.107$ |
| MRST02(LO, lo2002.dat) | $\Lambda_4^{\rm LO} = 220$ MeV | $\alpha_s^{\rm LO}(M_Z) = 0.125$ |
| MRST01(NLO, alf119.dat) | $\Lambda_4^{\rm NLO} = 323$ MeV | $\alpha_s^{\rm NLO}(M_Z) = 0.113$ |
| MRST02(NNLO, vnval1155.dat) | $\Lambda_4^{\rm NLO} = 235$ MeV | $\alpha_s^{\rm NNLO}(M_Z) = 0.109$ |

Table 1: Polarized and unpolarized parton density sets with the values for the QCD scale $\Lambda_4$ and the running coupling $\alpha_s(M_Z)$.

will only choose NLO polarized parton densities with the two-loop running coupling constant. The details are given in Table 1. Further we put $n_f = 4$ in the coefficient functions and the running coupling constants and the densities are only presented for the u,d,s and g partons. Finally we also make a comparison with unpolarized Drell-Yan production. For this cross section we adopt for LO the MRST02 [29] densities, for NLO the MRST01 [30] densities and for NNLO the approximate MRST02 [29] densities, with one, two and three loop running coupling constants respectively.

In Fig. 4 we have plotted the polarized Drell-Yan cross section in Eq. (4.1) up to NLO. It is clear that the $q\bar{q}$ contribution dominates the $qg$ contribution. The former is negative above $Q = 25$ GeV, while the latter is already negative in a region above $Q$=13 GeV. This implies that the total NLO contribution is actually negative above $Q$=27 GeV where it is very small. For this reason we have plotted the absolute values of the contributions in Fig. 4.

The relative sizes are not changed if we go to NNLO as demonstrated in Fig.5. Again the $q\bar{q}$ contribution is negative above $Q$= 25 GeV and the $qg$ contribution is negative between $Q$= 4 GeV and $Q$= 13 GeV. Here the $qq$ and $gg$ channels appear for the first time and they are both negative. However their contribution is negligible compared with the one given by $qg$ and certainly by the $q\bar{q}$ result. Again we have plotted the absolute values

of the contributions. We conclude that via the $q\bar{q}$ subprocess the sea-quark contribution dominates the whole cross section in proton-proton collisions irrespective of the value taken by the gluon density.

In Fig. 6 we have plotted the absolute values of the LO, NLO and NNLO polarized cross sections for $2 < Q < 30$ GeV. Notice that we are in the range of small $Q$-values so the $K$-factors are pretty large. We have defined the $K$-factors as

$$K^{\rm NLO} = \frac{\Delta\sigma^{\rm NLO}}{\Delta\sigma^{\rm LO}}\,, \qquad K^{\rm NNLO} = \frac{\Delta\sigma^{\rm NNLO}}{\Delta\sigma^{\rm LO}}\,, \tag{4.3}$$

and plotted them in Fig. 7. At $Q = 7$ GeV the K-factors reach a minimum, $K^{\rm NLO} \sim 1.2$ and $K^{\rm NNLO} \sim 1.3$, and at larger $Q$ they rise again. The rapid rise above $Q$= 18 GeV is due to the change in sign of the LO process near $Q$=25 GeV where the ratio is infinite. However the magnitude of the polarized cross section is extremely small in this region.

Next we turn to the variation of the cross section w.r.t. scale $\mu$. In Figs. 8a, 8b and 8c we show the LO, NLO and NNLO polarized cross sections at the scales $\mu = Q/2$, $\mu = Q$ and $\mu = 2Q$. In each figure we see that if $\mu$ gets larger the cross sections increase at small $Q$ but decrease it at larger $Q$. Therefore there are specific values in $Q$ where the scale variations are small and as we go from LO to NLO to NNLO these points are at larger values of $Q$. The scale variation gets smaller as we go from LO to NLO as expected. In spite of the fact that we do not have the NNLO parton densities there is still an improvement in the scale dependence if we go from NLO to NNLO. The corresponding plots for the unpolarized cross section are shown in Figs. 9a, 9b and 9c. These plots also show that when $\mu$ becomes large the cross sections increase at small $Q$ and decrease it at larger $Q$. Further we see the expected overall decrease in scale variation as we go from LO to NLO and then to NNLO.

To show the scale variation from a different point of view we plot the following quantity

$$N\left(\frac{\mu}{\mu_0}\right) = \frac{\Delta\sigma(\mu)}{\Delta\sigma(\mu_0)}\,. \tag{4.4}$$

In Fig. 10a we plot the polarized quantity in Eq. (4.4) for $0.4 < \mu/\mu_0 < 2$ at $\mu_0 = Q = 5$ GeV. In this figure we see an improvement in the scale variation

while going from LO to NLO and then to NNLO. This feature also persists at higher $Q$-values i.e. $Q = 10$ GeV in Fig. 10b and $Q = 15$ GeV in Fig. 10c. For the unpolarized cross section the trend is the same. Here we have the NNLO parton densities and in Fig. 11a at $Q = 5$ GeV we see an improvement in scale variation while going to higher order. The same observation can be made in Fig. 11b at $Q = 10$ GeV. However for $Q = 15$ GeV in Fig. 11c the NLO curve becomes slightly worse than the LO one. While on the other hand the NNLO curve is slightly better than the LO at least for larger scales $\mu$.

Now we look at effect of the higher order corrections on the longitudinal asymmetry defined by

$$A_{LL} = \frac{\Delta\sigma}{\sigma}\,. \tag{4.5}$$

In Fig. 12 we have plotted $A_{LL}$ in percent for BB1 in the range $2 < Q < 30$ GeV in LO, NLO and NNLO. Since the polarized cross section changes sign we see that the asymmetry is negative for large $Q$ (note the displaced zero). It is obvious that the longitudinal asymmetry is small reaching about one percent between $Q = 10$ GeV and $Q = 20$ GeV.

To show the predictions of the various polarized parton density sets we compare the BB1 NLO contribution with the other three NLO parton density sets i.e. BB2, GRSV01 (standard scenario or SS) and GRSV01 (valence scenario or VS) in Fig 13. Obviously the first three sets have small positive longitudinal asymmetries while the GRSV01 valence scenario set has a large negative asymmetry. Therefore the set with the smallest gluon, here GRSV01 (valence scenario), has the largest asymmetry. On the other hand the set with the largest gluon, here BB1, has the smallest asymmetry. This feature is unchanged in NNLO as can be seen in Fig. 14. Hopefully the RHIC experiments will get sufficient luminosities and large enough proton polarizations to distinguish between the first three predictions and the last one.

To summarize we have computed the NNLO corrections to the production of massive lepton-pairs in polarized proton-proton collisions. Hence as far as coefficient functions as concerned we have the NNLO corrections to both polarized and unpolarized processes. Unfortunately the corresponding anomalous dimensions of the partons are not available at NNLO. While fits have been made in the unpolarized case it is not possible yet in the polarized

case. Therefore we have convoluted the NLO polarized densities with the NNLO coefficient functions to get an idea of the stability of the perturbation series. First we have seen that the dominance of the sea-quark initiated process, which holds at LO and NLO, also prevails at NNLO. For the unpolarized cross section we have shown that the addition of the NNLO terms produces a significant reduction in the scale variation of the cross section. However the same phenomenon is also shown for the polarized cross section in spite of the fact that the NNLO parton densities are not known yet. Finally the longitudinal asymmetry is small and positive for the polarized parton density sets BB1, BB2 and GRSV(SS). If one uses the GRSV(VS) densities then the longitudinal polarization is negative and large.

# Appendix A

The lowest order contribution originating from the Born reaction Eq. (3.1) is given by

$$\Delta_{q\bar{q}}^{(0)} = -\delta(1-z)\,. \tag{A.1}$$

The $O(\alpha_s)$ correction to the $q\bar{q}$ subprocess in Eq. (3.2) has been calculated in the literature [8]-[11]. Choosing the $\overline{\rm MS}$ scheme the expression for $\Delta_{q\bar{q}}^{(1)}$ can be obtained by using $n$-dimensional regularization. For convenience we split the contribution as follows

$$\Delta_{q\bar{q}}^{(1)}(z) = \Delta_{q\bar{q}}^{(1),\rm S+V}(z) + \Delta_{q\bar{q}}^{(1),\rm H}(z)\,. \tag{A.2}$$

Here S+V indicates that the corrections are coming from soft-plus-virtual gluons where H means that the corrections are coming from the hard $z \neq 1$ gluon region. The expressions are equal to

$$\begin{aligned}\Delta_{q\bar{q}}^{(1),\rm S+V} &= -a_s\,C_F\left\{\delta(1-z)\Big[6\,\ln\left(\frac{Q^2}{\mu^2}\right) + 8\,\zeta(2) - 16\Big]\right.\\ &\left. +8\,\mathcal{D}_0(z)\,\ln\left(\frac{Q^2}{\mu^2}\right) + 16\,\mathcal{D}_1(z)\right\},\end{aligned} \tag{A.3}$$

$$\begin{aligned}\Delta_{q\bar{q}}^{(1),\rm H} &= a_s\,C_F\left\{4(1+z)\,\ln\left(\frac{Q^2}{\mu^2}\right) + 8(1+z)\,\ln(1-z)\right.\\ &\left. +4\frac{1+z^2}{1-z}\,\ln z\right\}\end{aligned} \tag{A.4}$$

where the distibutions $\mathcal{D}_i(z)$ are defined in Eq. (3.22). The second order correction to the non-singlet part $\Delta_{q\bar{q}}^{(2)}$ is determined by process in Eq. (3.4) and the higher order corrections to processes in Eq. (3.1) and Eq. (3.2). It can be split into two parts. The first piece is related through mass factorization to the collinearly singular part of the partonic structure function $W_{q\bar{q}}$ and will be denoted by

$$\Delta_{\bar{q}}^{(2),\rm NS} = \Delta_{q\bar{q}}^{(2),\rm S+V} + \Delta_{q\bar{q}}^{(2),\rm C_A} + \Delta_{q\bar{q}}^{(2),\rm C_F} + \Delta_{q\bar{q},A\bar{A}}^{(2)} + \Delta_{q\bar{q},A\bar{C}}^{(2)} + \Delta_{q\bar{q},A\bar{D}}^{(2)}\,. \tag{A.5}$$

The second piece consists of the DY correction terms $\Delta^{(2)}_{q\bar{q},B\bar{B}}$, $\Delta^{(2)}_{q\bar{q},B\bar{C}}$, $\Delta^{(2)}_{q\bar{q},B\bar{D}}$. The contribution $\Delta^{(2)}_{q\bar{q},A\bar{B}}$ is zero because of Furry's theorem. First we will enumerate the contributions in Eq. (A.5). The soft-plus-virtual gluon contributions come from the two-loop virtual graphs contributing to the Born reaction in Eq. (3.1), the soft gluon corrections to the reactions in Eqs. (3.2), (3.4) and soft quark pair production due to diagrams A in Fig. 1. The expression for this part is equal to

$$
\begin{aligned}
\Delta^{(2),S+V}_{q\bar{q}} \;=\; & -a_s^2\,\delta(1-z)\,\Bigg\{C_A\,C_F\,\Bigg[-11\ln^2\left(\frac{Q^2}{\mu^2}\right)+\Big[\frac{193}{3}\\
& -24\;\zeta(3)\Big]\ln\left(\frac{Q^2}{\mu^2}\right)-\frac{12}{5}\;\zeta(2)^2+\frac{592}{9}\;\zeta(2)+28\zeta(3)-\frac{1535}{12}\Bigg]\\
& +C_F^2\,\Bigg[\Big[18-32\;\zeta(2)\Big]\ln^2\left(\frac{Q^2}{\mu^2}\right)+\Big[24\zeta(2)+176\zeta(3)\\
& -93\Big]\ln\left(\frac{Q^2}{\mu^2}\right)+\frac{8}{5}\;\zeta(2)^2-70\;\zeta(2)\\
& -60\;\zeta(3)+\frac{511}{4}\Bigg]+n_f\,C_F\,\Bigg[2\ln^2\left(\frac{Q^2}{\mu^2}\right)-\frac{34}{3}\ln\left(\frac{Q^2}{\mu^2}\right)\\
& +8\;\zeta(3)-\frac{112}{9}\;\zeta(2)+\frac{127}{6}\Bigg]\Bigg\}+C_A\,C_F\,\Bigg[-\frac{44}{3}\;\mathcal{D}_0(z)\ln^2\left(\frac{Q^2}{\mu^2}\right)\\
& +\Bigg[\Big[\frac{536}{9}-16\;\zeta(2)\Big]\;\mathcal{D}_0(z)-\frac{176}{3}\;\mathcal{D}_1(z)\Bigg]\ln\left(\frac{Q^2}{\mu^2}\right)-\frac{176}{3}\;\mathcal{D}_2(z)\\
& +\Big[\frac{1072}{9}-32\;\zeta(2)\Big]\;\mathcal{D}_1(z)+\Big[56\zeta(3)+\frac{176}{3}\;\zeta(2)-\frac{1616}{27}\Big]\\
& \times\mathcal{D}_0(z)\Bigg]+C_F^2\,\Bigg[\Big[64\;\mathcal{D}_1(z)+48\;\mathcal{D}_0(z)\Big]\ln^2\left(\frac{Q^2}{\mu^2}\right)
\end{aligned}
$$

$$+\Big[192\ \mathcal{D}_2(z) + 96\ \mathcal{D}_1(z) - (128 + 64\ \zeta(2))\ \mathcal{D}_0(z)\Big] \ln\left(\frac{Q^2}{\mu^2}\right)$$

$$+128\ \mathcal{D}_3(z) - (128\ \zeta(2) + 256)\ \mathcal{D}_1(z) + 256\zeta(3)\ \mathcal{D}_0(z)\Bigg]$$

$$+n_f\, C_F \left[\frac{8}{3}\ \mathcal{D}_0(z) \ln^2\left(\frac{Q^2}{\mu^2}\right) + \left[\frac{32}{3}\ \mathcal{D}_1(z) - \frac{80}{9}\ \mathcal{D}_0(z)\right]\right.$$

$$\times \ln\left(\frac{Q^2}{\mu^2}\right) + \frac{32}{3}\ \mathcal{D}_2(z) - \frac{160}{9}\ \mathcal{D}_1(z)$$

$$\left.+(\frac{224}{27} - \frac{32}{3}\ \zeta(2))\ \mathcal{D}_0(z)\right]. \tag{A.6}$$

The hard gluon contribitions are denoted by $\Delta_{q\bar{q}}^{(2),\mathrm{C_A}}$ and $\Delta_{q\bar{q}}^{(2),\mathrm{C_F}}$. They are equal to

$$\begin{aligned}
\Delta_{q\bar{q}}^{(2),C_A} \;=\; & -a_s^2\, C_A\, C_F \left\{ \frac{22}{3}(1+z) \ln^2\left(\frac{Q^2}{\mu^2}\right) + \left[\frac{1+z^2}{1-z}\Big[ - 8\mathrm{Li}_2(1-z)\right.\right. \\
& +\frac{70}{3}\ln(z)\Big] + (1+z)\Big[8\zeta(2) + \frac{88}{3}\ln(1-z) - 6\ln(z)\Big] - \frac{4}{9}\big(19 \\
& \left.\left.+124z\big)\right] \ln\left(\frac{Q^2}{\mu^2}\right) + \frac{1+z^2}{1-z}\Big[ - 4\mathrm{S}_{1,2}(1-z) - 12\mathrm{Li}_3(1-z) \\
& +\frac{4}{3}\mathrm{Li}_2(1-z) + 8\mathrm{Li}_2(1-z)\ln(z) - 8\mathrm{Li}_2(1-z)\ln(1-z) \\
& +8\zeta(2)\ln(z) - \frac{29}{2}\ln^2(z) - \frac{104}{3}\ln(z) + \frac{140}{3}\ln(z)\ln(1-z)\Big] \\
& +(1+z)\Big[16\mathrm{S}_{1,2}(1-z) - 12\mathrm{Li}_3(1-z) - 28\zeta(3) \\
& +8\mathrm{Li}_2(1-z)\ln(1-z) + 16\zeta(2)\ln(1-z) + \frac{88}{3}\ln^2(1-z)
\end{aligned}$$

$$+\frac{23}{6}\ln^2(z) - 12\ln(z)\ln(1-z)\Big]$$

$$-\frac{4}{3}(7+13z)\mathrm{Li}_2(1-z) - \frac{4}{3}(19+25z)\zeta(2) - \frac{2}{3}(26-57z)\ln(z)$$

$$-\frac{4}{9}(38+239z)\ln(1-z) - \frac{446}{27} + \frac{2278}{27}z\Big\}, \qquad \text{(A.7)}$$

and

$$\begin{aligned}
\Delta_{q\bar{q}}^{(2),C_F} \;=\; & -a_s^2\, C_F^2 \Big\{ \Big[ -16\frac{1+z^2}{1-z}\ln(z) + 8(1+z)\Big[\ln(z) - 4\ln(1-z)\Big] \\
& -8(5+z)\Big]\ln^2\left(\frac{Q^2}{\mu^2}\right) + \Big[\frac{1+z^2}{1-z}\Big[16\mathrm{Li}_2(1-z) + 24\ln^2(z) \\
& -24\ln(z) - 112\ln(z)\ln(1-z)\Big] + (1+z)\Big[32\mathrm{Li}_2(1-z) \\
& +32\zeta(2) - 12\ln^2(z) + 32\ln(z)\ln(1-z) - 96\ln^2(1-z)\Big] \\
& +8(15+2z) + 16(2-3z)\ln(z) - 16(7-z)\ln(1-z)\Big] \\
& \times \ln\left(\frac{Q^2}{\mu^2}\right) + \frac{1+z^2}{1-z}\Big[ -32\mathrm{S}_{1,2}(1-z) - 8\mathrm{Li}_3(1-z) \\
& -24\mathrm{Li}_2(1-z)\ln(z) + 24\mathrm{Li}_2(1-z)\ln(1-z) - 12\ln^3(z) \\
& +64\zeta(2)\ln(z) + 72\ln^2(z)\ln(1-z) - 124\ln^2(1-z)\ln(z) \\
& +56\ln(z)\Big] + (1-z)\Big[64\zeta(2) - 64\ln^2(1-z)\Big] \\
& +(1+z)\Big[\frac{14}{3}\ln^3(z) - 64\ln^3(1-z) - 40\mathrm{Li}_3(1-z) \\
& +48\mathrm{Li}_2(1-z)\ln(1-z) - 32\zeta(2)\ln(z) + 16\mathrm{S}_{1,2}(1-z)
\end{aligned}$$

$$+64\zeta(2)\ln(1-z) - 128\zeta(3) - 24\ln^2(z)\ln(1-z)$$

$$+32\ln^2(1-z)\ln(z)\Big] - 8(3+4z)\mathrm{Li}_2(1-z)$$

$$-8(1-3z)\ln^2(z) + 16(4-7z)\ln(z)\ln(1-z)$$

$$-8(6-13z)\ln(z) + 4(64+3z)\ln(1-z) - 24(3-2z)\Big\}. \quad \text{(A.8)}$$

The function $\mathrm{Li}_n(z)$ and $\mathrm{S}_{n,p}(z)$ denote the polylogarithms and can be found in [31]. The hard part of quark pair production due to the diagrams A in Fig. 1 is equal to

$$\begin{aligned}
\Delta^{(2)}_{q\bar{q},A\overline{A}} &= -a_s^2\, n_f\, C_F \Bigg\{ -\frac{4}{3}(1+z)\ln^2\left(\frac{Q^2}{\mu^2}\right) + \Bigg[ -\frac{16}{3}\frac{1+z^2}{1-z} \\
&\quad \times \ln(z) - \frac{16}{3}(1+z)\ln(1-z) - \frac{8}{9}(1-11z)\Bigg]\ln\left(\frac{Q^2}{\mu^2}\right) \\
&\quad + \frac{1+z^2}{1-z}\Bigg[4\ln^2(z) - \frac{4}{3}\mathrm{Li}_2(1-z) + \frac{20}{3}\ln(z) \\
&\quad - \frac{32}{3}\ln(z)\ln(1-z)\Bigg] + (1+z)\Bigg[\frac{4}{3}\mathrm{Li}_2(1-z) \\
&\quad + \frac{16}{3}\zeta(2) - \frac{16}{3}\ln^2(1-z) + \frac{2}{3}\ln^2(z)\Bigg] - \frac{16}{9}\Big(1-11z\Big) \\
&\quad \times \ln(1-z) + \frac{8}{3}\Big(2-3z\Big)\ln(z) + \frac{4}{27}\Big(47-103z\Big)\Bigg\}, \qquad \text{(A.9)}
\end{aligned}$$

Finally, we have the interference terms corresponding to the combinations $A\bar{C}$ and $A\bar{D}$ in Fig. 1 and Fig. 2. For them we find

$$\Delta^{(2)}_{q\bar{q},A\overline{C}} = \Delta^{(2)}_{q\bar{q},A\overline{D}} = -a_s^2\, C_F\, \left(C_F - \frac{1}{2}\, C_A\right)\, \Bigg\{\Bigg[\frac{1+z^2}{1-z}\Bigg[ - 8\mathrm{Li}_2(1-z)$$

$$
-4\ln^2(z) - 6\ln(z)\Big] - 14(1+z)\ln(z) - 4(8-7z)\Big]\ln\left(\frac{Q^2}{\mu^2}\right)
$$

$$
+\frac{1+z^2}{1-z}\Big[16\mathrm{Li}_3(1-z) - 36\mathrm{S}_{1,2}(1-z) + \frac{8}{3}\ln^3(z)
$$

$$
-12\mathrm{Li}_2(1-z)\ln(z) - 16\mathrm{Li}_2(1-z)\ln(1-z)
$$

$$
-6\mathrm{Li}_2(1-z) + \frac{15}{2}\ln^2(z) - 8\ln^2(z)\ln(1-z)
$$

$$
+12\ln(z) - 12\ln(z)\ln(1-z)\Big] + (1+z)\Big[-8\mathrm{Li}_3(1-z)
$$

$$
-26\mathrm{Li}_2(1-z) + 4\mathrm{Li}_2(1-z)\ln(z) + \frac{2}{3}\ln^3(z) + \frac{23}{2}\ln^2(z)
$$

$$
-28\ln(z)\ln(1-z)\Big] + 2(22-9z)\ln(z) - 8(8-7z)\ln(1-z)
$$

$$
+2(47-39z)\Big\}\,. \tag{A.10}
$$

The remaining parts of $q\bar{q}$ scattering are free of mass singularities. Therefore they do not need mass factorization, which implies that their contributions are scheme and scale independent. The contributions from the diagrams B in Fig. 1 and the interference terms $B\bar{C}$ and $B\bar{D}$ (see Figs. 1, 2) are

$$
\begin{aligned}
\Delta^{(2)}_{q\bar{q},B\overline{B}} &= -a_s^2\,T_f\,C_F\Big\{(1+z)^2\Big[-\frac{32}{3}\mathrm{Li}_2(-z) - \frac{16}{3}\zeta(2) + \frac{8}{3}\ln^2(z) \\
&\quad -\frac{32}{3}\ln(z)\ln(1+z)\Big] + \frac{8}{3}\Big(3+3z^2+4z\Big)\ln(z) \\
&\quad +\frac{40}{3}\Big(1-z^2\Big)\Big\}\,,
\end{aligned} \tag{A.11}
$$

and

$$
\Delta^{(2)}_{q\bar{q},B\overline{C}} = \Delta^{(2)}_{q\bar{q},B\overline{D}} = -a_s^2\,C_F\,\Big(C_F - \frac{1}{2}\,C_A\Big)\,\Big\{(1+z^2+3z)
$$

$$\times\Big[32\mathrm{S}_{1,2}(1-z)+16\mathrm{Li}_2(1-z)\ln(z)\Big]+(1+z)^2\Big[-48\mathrm{S}_{1,2}(-z)$$

$$-8\mathrm{Li}_3(-z)+24\mathrm{Li}_2(-z)+24\mathrm{Li}_2(-z)\ln(z)$$

$$-48\mathrm{Li}_2(-z)\ln(1+z)+12\zeta(2)-24\zeta(2)\ln(1+z)$$

$$+8\zeta(2)\ln(z)+20\ln^2(z)\ln(1+z)-24\ln^2(1+z)$$

$$\times\ln(z)+24\ln(z)\ln(1+z)\Big]+36(1-z^2)\mathrm{Li}_2(1-z)$$

$$+\frac{4}{3}\Big(1+z^2+4z\Big)\ln^3(z)+4(9+11z)\ln(z)-2(-6$$

$$+15z^2+8z)\ln^2(z)-2(-27+13z^2+14z)\Big\}. \tag{A.12}$$

Because of Furry's theorem

$$\Delta^{(2)}_{q\bar{q},A\overline{B}}=0\,. \tag{A.13}$$

At $\mathrm{O}(\alpha_s)$ the $qg$ subprocess shows up for the first time. The Drell-Yan correction term for the reaction in Eq. (3.3) has been calculated in [8], [9], [10], [11] and it is given by

$$\Delta^{(1)}_{qg}=-a_s\,T_f\left\{\Big[4\,z-2\Big]\,\ln\left(\frac{(1-z)^2\,Q^2}{z\,\mu^2}\right)+(1-z)(5+3\,z)\right\}. \tag{A.14}$$

The second order part of $\Delta_{qg}$ receives contributions from the virtual corrections to the reaction in Eq. (3.3) and the process in Eq. (3.5)

$$\Delta^{(2)}_{qg}=\Delta^{(2)}_{\bar{q}g}=\Delta^{(2),\mathrm{C_A}}_{qg}+\Delta^{(2),\mathrm{C_F}}_{qg}\,. \tag{A.15}$$

The calculation of $\Delta^{(2)}_{qg}$ requires both mass factorization and renormalization. The two parts $\Delta^{(2),\mathrm{C_A}}_{qg}$ and $\Delta^{(2),\mathrm{C_F}}_{qg}$ are equal to

$$\Delta^{(2),C_A}_{qg} \;=\; a_s^2\,C_A\,T_f\left\{\Big[-8(1+z)\ln(z)+4(1-2z)\ln(1-z)\right.$$

$$-24(1-z)\Big]\ln^2\left(\frac{Q^2}{\mu^2}\right)+\Big[8(1+2z)\Big[\mathrm{Li}_2(-z)$$

$$+\ln(z)\ln(1+z)-3\mathrm{Li}_2(1-z)\Big]+4(3+4z)\ln^2(z)$$

$$-8(1-4z)\zeta(2)-8(5+2z)\ln(z)\ln(1-z)+12(1-2z)$$

$$\times\ln^2(1-z)-4(25-22z-3z^2)\ln(1-z)$$

$$+4(13-22z-3z^2)\ln(z)$$

$$+4(17-18z)\Big]\ln\left(\frac{Q^2}{\mu^2}\right)-24(1+z)\Big[\mathrm{Li}_2(-z)$$

$$+\ln(z)\ln(1+z)\Big]+4(1+2z)\Big[2\mathrm{Li}_3(-z)$$

$$+4\mathrm{Li}_3\left(-\frac{1-z}{1+z}\right)-4\mathrm{Li}_3\left(\frac{1-z}{1+z}\right)-4\ln(z)\mathrm{Li}_2(-z)$$

$$+4\ln(1-z)\mathrm{Li}_2(-z)-3\ln^2(z)\ln(1+z)+4\ln(z)$$

$$\times\ln(1-z)\ln(1+z)\Big]-8(11+12z)\mathrm{S}_{1,2}(1-z)$$

$$+4(19+26z)\mathrm{Li}_3(1-z)+8(1+z)\zeta(3)-8(4-z)\ln(z)$$

$$\times\mathrm{Li}_2(1-z)-48(1+2z)\ln(1-z)\mathrm{Li}_2(1-z)$$

$$+4(-29+8z-6z^2)\mathrm{Li}_2(1-z)+40\zeta(2)\ln(z)$$

$$-16(1-4z)\zeta(2)\ln(1-z)+4(29-38z+3z^2)\zeta(2)$$

$$-\frac{2}{3}(11+16z)\ln^3(z)+\frac{26}{3}(1-2z)\ln^3(1-z)$$

$$+(-47+92z+12z^2)\ln^2(z)+4(7+6z)\ln^2(z)\ln(1-z)$$

$$-4(11+2z)\ln(z)\ln^2(1-z)+4(-26+23z+3z^2)$$

$$\times \ln^2(1-z) + 4(-36+35z)\ln(z) + 4(27-44z-9z^2)$$
$$\times \ln(z)\ln(1-z) + 2(-72+71z+3z^2)$$
$$+2(68-71z)\ln(1-z)\Big\}, \qquad \text{(A.16)}$$

and

$$\begin{aligned}
\Delta_{qg}^{(2),C_F} &= a_s^2\, C_F\, T_f \Big\{ \Big[12(1-2z)\ln(1-z) - 6(1-2z)\ln(z) \\
&-9\Big]\ln^2\left(\frac{Q^2}{\mu^2}\right) + \Big[4(1-2z)\Big[9\ln^2(1-z) - 2\zeta(2) + 2\ln^2(z) \\
&-10\ln(z)\ln(1-z)\Big] + 2(29-8z-6z^2)\ln(z) \\
&+6(-16+12z+2z^2)\ln(1-z) + 2(49-38z)\Big] \\
&\times \ln\left(\frac{Q^2}{\mu^2}\right) + 32(1+z)\Big[\mathrm{Li}_2(-z) + \ln(z)\ln(1+z)\Big] \\
&+2(1-2z)\Big[16\mathrm{Li}_3(-z) + 50\zeta(3) \\
&-8\mathrm{Li}_2(-z)\ln(z) - 8\zeta(2)\ln(1-z) \\
&+\frac{35}{3}\ln^3(1-z)\Big] - 12(1-2z)\mathrm{S}_{1,2}(1-z) - 20(1-2z) \\
&\times \mathrm{Li}_3(1-z) + 4(1-2z)\ln(z)\mathrm{Li}_2(1-z) + 4(1-2z) \\
&\times \ln(1-z)\mathrm{Li}_2(1-z) + 2(13+28z)\mathrm{Li}_2(1-z) \\
&+24(1-2z)\zeta(2)\ln(z) + 4(1+10z-6z^2)\zeta(2) \\
&-\frac{17}{3}(1-2z)\ln^3(z) + 24(1-2z)\ln(1-z)\ln^2(z)
\end{aligned}$$

$$
\begin{aligned}
&+(-\frac{81}{2} - 20z + 6z^2)\ln^2(z) - 42(1-2z)\ln^2(1-z)\ln(z) \\
&+2(-55 + 52z + 9z^2)\ln^2(1-z) + 4(35 - 12z - 6z^2) \\
&\times \ln(z)\ln(1-z) + (-175 + 79z + 60z^2)\ln(z) \\
&-2(-128 + 77z + 30z^2)\ln(1-z) - \frac{627}{2} + 331z - \frac{15}{2}z^2\Big\}.
\end{aligned}
\tag{A.17}
$$

The reactions in Fig. 2 describe quark-anti-quark as well as quark-quark scattering (without identical quarks). The contribution to the DY correction term can be split into two parts. The first part, represented by the combinations $C\bar{C}$ and $D\bar{D}$ needs mass factorization. In this case the contributions for $q\bar{q}$, $qq$ and $\bar{q}\bar{q}$ are all equal and are given by

$$
\begin{aligned}
\Delta^{(2)}_{q\bar{q},C\overline{C}} &= \Delta^{(2)}_{q\bar{q},D\overline{D}} = \Delta^{(2)}_{qq,C\overline{C}} = \Delta^{(2)}_{qq,D\overline{D}} = \Delta^{(2)}_{\bar{q}\bar{q},C\overline{C}} = \Delta^{(2)}_{\bar{q}\bar{q},D\overline{D}} = \\
&a_s^2\, C_F\, T_f \Big\{ \Big[ -4(1+z)\ln(z) - 10(1-z)\Big]\ln^2\left(\frac{Q^2}{\mu^2}\right) \\
&+\Big[8(1+z)\Big[ -2\mathrm{Li}_2(1-z) + \ln^2(z) - 2\ln(z)\ln(1-z)\Big] \\
&+4(7-8z)\ln(z) - 40(1-z)\ln(1-z) + 40(1-z)\Big] \\
&\times \ln\left(\frac{Q^2}{\mu^2}\right) - 40(1-z)\Big[\ln^2(1-z) - \zeta(2)\Big] + 8(1+z) \\
&\times\Big[ -6\mathrm{S}_{1,2}(1-z) + 4\mathrm{Li}_3(1-z) - \ln(z)\mathrm{Li}_2(1-z) \\
&-4\ln(1-z)\mathrm{Li}_2(1-z) + 2\zeta(2)\ln(z) - \frac{3}{4}\ln^3(z) \\
&+2\ln^2(z)\ln(1-z) - 2\ln(z)\ln^2(1-z)\Big] - 4(9-7z) \\
&\times\mathrm{Li}_2(1-z) + 8(7-8z)\ln(z)\ln(1-z) + (-25+39z)
\end{aligned}
$$

$$\times \ln^2(z) + 80(1-z)\ln(1-z) + 2(-42+17z)\ln(z)$$

$$-131 + 128z + 3z^2 \Big\}. \qquad \text{(A.18)}$$

The second part, which is collinearly finite, consists of the interference between the graphs C and D in Fig. 2. Further notice the relative minus sign between the $q\bar{q}$ and the $qq$ ($\bar{q}\bar{q}$) part. The expresions for these interference terms are

$$\begin{aligned}
\Delta^{(2)}_{q\bar{q}C\overline{D}} &= -\Delta^{(2)}_{qqC\overline{D}} = -\Delta^{(2)}_{\bar{q}\bar{q}C\overline{D}} = \\
& a_s^2\, C_F\, T_f \Big\{ 8(2+z)\Big[ -4\mathrm{S}_{1,2}(1-z) + 12\mathrm{S}_{1,2}(-z) \\
& +6\ln^2(1+z)\ln(z) + 6\zeta(2)\ln(1+z) - 5\ln(1+z)\ln^2(z) \\
& +12\ln(1+z)\mathrm{Li}_2(-z)\Big] - 8(1+z)\Big[2\mathrm{Li}_2(-z) + 2\ln(z)\ln(1+z) \\
& +\zeta(2)\Big] - 8(2-z)\mathrm{Li}_3(1-z) + 16(6-5z)\mathrm{Li}_3(-z) \\
& +8(6-9z)\zeta(3) - 8(2+3z)\mathrm{Li}_2(1-z)\ln(z) + \frac{16}{3}z\ln^3(z) \\
& -128\ln(z)\mathrm{Li}_2(-z) - 8(2+5z)\zeta(2)\ln(z) - 8\mathrm{Li}_2(1-z) \\
& +4z\ln^2(z) + 16\ln(z) + 32(1-z) \Big\}. \qquad \text{(A.19)}
\end{aligned}$$

In case there are identical quarks in the final state, we have in addition to the graphs in Fig. 2 also the ones in Fig. 3. As the results for $E\bar{E}$, $F\bar{F}$ and $E\bar{F}$ are equal to those for $C\bar{C}$, $D\bar{D}$ and $C\bar{D}$ (of course one has to implement the right statistical factors), we will not discuss them here. The new contributions come from the intereference terms $C\bar{E}$, $C\bar{F}$, $D\bar{E}$ and $D\bar{F}$. Further when the intermediate vector boson is a photon all four sets of diagrams C,D,E and F contribute and we have a statistical factor 1/2. Apart from the statistical factor there is another difference bewtween $C\bar{E}$ ($D\bar{F}$) and $C\bar{F}$ ($D\bar{E}$). The first contains collinear divergences and needs mass

factorization, whereas the latter is free of mass singularities. The correction corresponding to the interferences $C\bar{E}$ and $D\bar{F}$ is equal to

$$
\begin{aligned}
\Delta^{(2)}_{qq,C\overline{E}} \;=\; & \Delta^{(2)}_{qq,D\overline{F}} = \Delta^{(2)}_{\bar{q}\bar{q},C\overline{E}} = \Delta^{(2)}_{\bar{q}\bar{q},D\overline{F}} = a_s^2 C_F \left(C_F - \frac{1}{2}C_A\right) \Bigg\{ \Bigg[ \frac{1+z^2}{1+z} \\
& \times \Bigg[ 4\ln^2(z) - 8\zeta(2) - 16\mathrm{Li}_2(-z) - 16\ln(z)\ln(1+z) \Bigg] \\
& + 8(1+z)\ln(z) + 16(1-z) \Bigg] \ln\left(\frac{Q^2}{\mu^2}\right) + \frac{1+z^2}{1+z} \\
& \times \Bigg[ 32\mathrm{S}_{1,2}(1-z) - 16\mathrm{S}_{1,2}(-z) - 32\mathrm{Li}_3(1-z) \\
& - 8\mathrm{Li}_3(-z) - 32\mathrm{Li}_3\left(-\frac{1-z}{1+z}\right) + 32\mathrm{Li}_3\left(\frac{1-z}{1+z}\right) - 4\zeta(3) \\
& + 24\mathrm{Li}_2(1-z)\ln(z) + 32\mathrm{Li}_2(-z)\ln(z) - 32\mathrm{Li}_2(-z)\ln(1-z) \\
& - 16\mathrm{Li}_2(-z)\ln(1+z) + 12\zeta(2)\ln(z) - 16\zeta(2)\ln(1-z) \\
& - 8\zeta(2)\ln(1+z) - \frac{8}{3}\ln^3(z) + 8\ln^2(z)\ln(1-z) \\
& + 28\ln^2(z)\ln(1+z) - 8\ln^2(1+z)\ln(z) - 32\ln(z)\ln(1-z) \\
& \times \ln(1+z) \Bigg] + (1-z) \Bigg[ - 16\mathrm{S}_{1,2}(-z) + 8\mathrm{Li}_3(-z) + 8\zeta(3) \\
& - 16\mathrm{Li}_2(-z)\ln(1+z) + 4\zeta(2)\ln(z) - 8\zeta(2)\ln(1+z) \\
& - \frac{2}{3}\ln^3(z) + 4\ln^2(z)\ln(1+z) - 8\ln^2(1+z)\ln(z) \\
& + 32\ln(1-z) - 34 \Bigg] + (1+z) \Bigg[ 8\mathrm{Li}_2(-z) + 4\zeta(2)
\end{aligned}
$$

$$+16\ln(z)\ln(1-z)+8\ln(z)\ln(1+z)\Big]+8(3+z)$$

$$\times\mathrm{Li}_2(1-z)-4(1+3z)\ln^2(z)-2(9-7z)\ln(z)\Big\}. \qquad \text{(A.20)}$$

The expression for the interference terms $C\bar{F}$ and $D\bar{E}$ is

$$\begin{aligned}\Delta^{(2)}_{qq,C\overline{F}} &= \Delta^{(2)}_{qq,D\overline{E}}=\Delta^{(2)}_{\bar{q}\bar{q},C\overline{F}}=\Delta^{(2)}_{\bar{q}\bar{q},D\overline{E}}= \\ & a_s^2\,C_F(C_F-\frac{1}{2}C_A)\Big\{(1-z)^2\Big[8\mathrm{Li}_3(1-z) \\ & -12\mathrm{Li}_2(1-z)-8\mathrm{Li}_2(1-z)\ln(z)-8\mathrm{S}_{1,2}(1-z) \\ & -\frac{4}{3}\ln^3(z)-6\ln^2(z)\Big]-2(7-6z)\ln(z) \\ & -(15+13z^2-28z)\Big\}. \qquad \text{(A.21)}\end{aligned}$$

Notice that the above expression is scheme and scale independent. The diagrams for the gluon-gluon subprocess can be obtained from the quark-anti-quark annihilation graphs via crossing. The subprocess shows up for the first time at $\mathrm{O}(\alpha_s^2)$. We have divided its Drell-Yan correction term into two parts i.e.

$$\Delta^{(2)}_{gg}=\Delta^{(2),\mathrm{C_A}}_{gg}+\Delta^{(2),\mathrm{C_F}}_{gg}\,. \qquad \text{(A.22)}$$

The $C_A$-contribution is collinearly finite and is therefore scheme and scale independent. It is given by

$$\begin{aligned}\Delta^{(2),C_A}_{gg} &= a_s^2\,\frac{N^2}{N^2-1}\Big\{-(1+z)^2\,\Big[16\mathrm{S}_{1,2}(-z)+24\mathrm{Li}_3(-z) \\ & +16\,\zeta(3)+\frac{16}{3}\,\mathrm{Li}_2(-z)-24\,\mathrm{Li}_2(-z)\ln(z) \\ & +16\mathrm{Li}_2(-z)\ln(1+z)+8\zeta(2)\ln(1+z)+\frac{8}{3}\zeta(2)\end{aligned}$$

$$
\begin{aligned}
&-12\ln^2(z)\ln(1+z) + 8\ln^2(1+z)\ln(z) + \frac{16}{3}\ln(z) \\
&\times \ln(1+z)\Big] - 8(1-z)^2 \mathrm{S}_{1,2}(1-z) + \Big(4 + \frac{124}{3}z + 22z^2\Big) \\
&\times \ln(z) + \Big(\frac{4}{3} - \frac{28}{3}z - \frac{14}{3}z^2\Big)\ln^2(z) + \frac{101}{3}(1-z^2)\Bigg\}. \quad \text{(A.23)}
\end{aligned}
$$

The $C_F$-contribution contains collinear singularities. After mass factorization in the $\overline{\rm MS}$-scheme we find

$$
\begin{aligned}
\Delta_{gg}^{(2),C_F} \;=\; & a_s^2 \Bigg\{ \Big[2(1+4z)\ln(z) + 8(1-z)\Big]\ln^2\left(\frac{Q^2}{\mu^2}\right) \\
&+\Big[2(1+4z)(4\ln(z)\ln(1-z) - \ln^2(z) + 4\mathrm{Li}_2(1-z)) \\
&+32(1-z)\ln(1-z) - 2(9-8z)\ln(z) - 43 + 52z - 9z^2\Big] \\
&\times \ln\left(\frac{Q^2}{\mu^2}\right) + 4(1+4z)\Big[ -4\mathrm{Li}_3(1-z) + \mathrm{Li}_2(1-z)\ln(z) \\
&+4\mathrm{Li}_2(1-z)\ln(1-z) - \ln^2(z)\ln(1-z) + 2\ln(z) \\
&\times \ln^2(1-z)\Big] - 8(1+z)\Big[\mathrm{Li}_2(-z) + \ln(z)\ln(1+z)\Big] \\
&+4(1+z)^2\Big[4\mathrm{S}_{1,2}(-z) + 4\mathrm{Li}_2(-z)\ln(1+z) \\
&+2\zeta(2)\ln(1+z) - 3\ln^2(z)\ln(1+z) + 2\ln^2(1+z) \\
&\times \ln(z)\Big] + 8(3+6z+z^2)\mathrm{S}_{1,2}(1-z) + 8(1+2z-z^2) \\
&\times \mathrm{Li}_3(-z) + 4(1+2z-2z^2)\zeta(3) + 4(3-4z)\mathrm{Li}_2(1-z) \\
&-8(2+4z+z^2)\ln(z)\mathrm{Li}_2(-z) - 4(3+10z+2z^2) \\
&\times \zeta(2)\ln(z) - 4(9-7z)\zeta(2) + 2(1+\frac{8}{3}z+\frac{4}{3}z^2)\ln^3(z)
\end{aligned}
$$

$$+2(7+3z)\ln^2 z + 32(1-z)\ln^2(1-z) - 4(9-8z)$$
$$\times \ln(z)\ln(1-z) + (55-72z+27z^2)\ln(z)$$
$$-2(43-52z+9z^2)\ln(1-z) + 2(35-31z-4z^2)\Big\}. \quad \text{(A.24)}$$

# References


[1] G. Bunce, N. Saito, J. Soffer, W. Vogelsang, Ann. Rev. Nucl. Part. Sci. 50 (2000) 525, hep-ph/0007218.

[2] E.L. Berger, L.E. Gordon, M. Klasen, Phys. Rev. D58 (1998) 074012, hep-ph/9803387.

[3] E.L. Berger, L.E. Gordon, M. Klasen, Phys. Rev. D62 (2000) 014014, hep-ph/9909446.

[4] V. Ravindran, J. Smith, W.L. van Neerven, Nucl. Phys. B647 (2002) 275, hep-ph/0207076.

[5] S. Chang, C. Coriano, R.D. Field, L.E. Gordon, Phys. Lett. B403 (1997) 344, hep-ph/9702252;
S. Chang, C. Coriano, R.D. Field, L.E. Gordon, Nucl. Phys. B512 (1998) 393, hep-ph/9705249.

[6] S. Chang, C. Coriano, R.D. Field, Nucl. Phys. B528 (1998) 285, hep-ph/9803280.

[7] P.G. Ratcliffe, Nucl. Phys. B223 (1983) 45.

[8] A. Weber, Nucl. Phys. B382 (1992) 63.

[9] P. Mathews, V. Ravindran, Mod. Phys. Lett. A7 (1992) 2695.

[10] T. Gehrmann, Nucl. Phys. B498 (1997) 245, hep-ph/9702263;
T. Gehrmann, Nucl. Phys. B534 (1998) 21, hep-ph/9710508.

[11] B. Kamal, Phys. Rev. D53 (1996) 1142, hep-ph/9511217;
B. Kamal, Phys. Rev. D57 (1998) 6663, hep-ph/9710374.

[12] G. 't Hooft, M. Veltman, Nucl. Phys. B44 (1972) 189.

[13] P. Breitenlohner, B. Maison, Commun. Math. 53 (1977) 11;
P. Breitenlohner, B. Maison, Commun. Math. 53 (1977) 39;
P. Breitenlohner, B. Maison, Commun. Math. 53 (1977) 55.

[14] S.L. Adler, W. Bardeen, Phys. Rev. 182 (1969) 1517.

[15] S.L. Adler, Phys. Rev. 177 (1969) 2426;
J.S Bell, R. Jackiw, Nuovo Cim. A60 (1969) 47.

[16] D. Akyeampong, R. Delbourgo, Nuov. Cim. 17A (1973) 578;
D. Akyeampong, R. Delbourgo, Nuov. Cim. 18A (1973) 94;
D. Akyeampong, R. Delbourgo, Nuov. Cim. 19A (1974) 219.

[17] C.G. Bollini, J.J. Giambiagi, Nucl. Phys. B97 (1975) 522, ibid. "Rio De Janiero 1974, Fifth Brazilian Symposium On Theoretical Physics, Vol. 1", Rio De Janiero 1975, 335;
M. Bos, Ann. Phys. (NY) 181 (1988) 177;
C. Schubert, Nucl. Phys. B323 (1989) 478;
C.P. Martin, D. Sanchez-Ruiz, Nucl. Phys. B572 (2000) 387, hep-th/0005076.

[18] J.A.M. Vermaseren, "New features of FORM", math-ph/0010025, version 3.0 available from http://www.nikhef.nl/form.

[19] S.A. Larin, Phys. Lett. B303 (1993) 113, hep-ph/9302240;
S.A. Larin, Phys. Lett. B334 (1994) 192, hep-ph/9403383.

[20] R. Mertig, W.L. van Neerven, Z. Phys. C70 (1996) 637, hep-ph/9506451.

[21] W. Vogelsang, Phys. Rev. D54 (1996) 2023, hep-ph/9512218;
W. Vogelsang, Nucl. Phys. B475 (1996) 47, hep-ph/9603366.

[22] W.L. van Neerven, Acta Phys. Polon. B29 (1998) 1175, hep-ph/9801325.

[23] Y. Matiounine, J. Smith, W.L. van Neerven, Phys. Rev. D58 (1998) 076002, hep-ph/9803439.

[24] T. Matsuura, S.C. van der Marck, W.L. van Neerven, Nucl. Phys. B319 (1989) 570.

[25] T. Matsuura, R. Hamberg, W.L. van Neerven, Nucl. Phys. B359 (1991) 343.

[26] A. Retey. J. Vermaseren, Nucl. Phys. B604 (2001) 281, hep-ph/0007294.

[27] J. Blümlein, H. Böttcher, Nucl. Phys. B636 (2002) 225, hep-ph/0203155.

[28] M. Glück, E. Reya, M. Stratmann, W. Vogelsang, Phys. Rev. D63 (2001) 094005, hep-ph/0011215.

[29] A.D. Martin, R.G. Roberts, W.J. Stirling, R.S. Thorne, Phys. Lett. B531 (2002) 216, hep-ph/0201127.

[30] A.D. Martin, R.G. Roberts, W.J. Stirling, R.S. Thorne, Eur. Phys. J. C23 (2002) 73, hep-ph/0110215.

[31] L. Lewin, "Polylogarithms and Associated Functions", North Holland, Amsterdam, 1983.

## Figure Captions

**Fig. 4.** The NLO differential cross section $d\Delta\sigma/dQ$ at $\sqrt{s} = 200$ GeV for the BB1 parton densities plotted in the range $2 < Q < 30$ GeV and $\mu^2 = Q^2$. The NLO plots are for the $O(\alpha_s)$ corrected $q\bar{q}$ (dot-dashed line), the $O(\alpha_s)$ contribution $qg$ (dashed line) and the total sum (solid line). Note that all contributions have negative regions at large $Q$ so we have plotted their absolute values (see text).

**Fig. 5.** Same as Fig. 4 but now for NNLO. Further we have shown the $O(\alpha_s^2)$ corrected $q\bar{q}$ (dot-dashed line), the $O(\alpha_s^2)$ corrected $qg$ (long-dashed line), the $O(\alpha_s^2)$ contributions $gg$ (dotted line) and $qq$ (short-dashed line) and the total sum (solid line). Note that all contributions have negative regions so we have plotted their absolute values (see text).

**Fig. 6.** The cross section $d\Delta\sigma/dQ$ at $\sqrt{s} = 200$ GeV plotted in range $2 < Q < 30$ GeV; LO (dotted line), NLO (dashed line), NNLO (solid line). Note that all contributions have negative regions at large $Q$ so we have plotted their absolute values (see text).

**Fig. 7.** The K-factor at $\sqrt{s} = 200$ GeV plotted in the region $2 < Q < 30$ GeV; $K^{\rm NLO}$ (dashed line), $K^{\rm NNLO}$ (solid line).

**Fig. 8a.** The cross section $d\Delta\sigma/dQ$ at $\sqrt{s} = 200$ GeV plotted in the region $2 < Q < 30$ GeV; LO $\mu = Q$ (solid line), LO $\mu = Q/2$ (dashed line) , LO $\mu = 2Q$ (dotted line).

**Fig. 8b.** The cross section $d\Delta\sigma/dQ$ at $\sqrt{s} = 200$ GeV plotted in the region $2 < Q < 30$ GeV. NLO $\mu = Q$ (solid line), NLO $\mu = Q/2$ (dashed line), NLO $\mu = 2Q$ (dotted line).

**Fig. 8c.** The cross section $d\Delta\sigma/dQ$ at $\sqrt{s} = 200$ GeV plotted in the region $2 < Q < 30$ GeV. NNLO $\mu = Q$ (solid line), NNLO $\mu = Q/2$ (dashed line), NNLO $\mu = 2Q$ (dotted line).

**Fig. 9a.** The unpolarized cross section $d\sigma/dQ$ at $\sqrt{s} = 200$ GeV plotted in the region $2 < Q < 30$ GeV. LO $\mu = Q$ (solid line), LO $\mu = Q/2$ (dashed line), LO $\mu = 2Q$ (dotted line).

**Fig. 9b.** The unpolarized cross section $d\sigma/dQ$ at $\sqrt{s} = 200$ GeV plotted in the region $2 < Q < 30$ GeV. NLO $\mu = Q$ (solid line), NLO $\mu = Q/2$ (dashed line), NLO $\mu = 2Q$ (dotted line).

**Fig. 9c.** The unpolarized cross section $d\sigma/dQ$ at $\sqrt{s} = 200$ GeV plotted in the region $2 < Q < 30$ GeV. NNLO $\mu = Q$ (solid line), NNLO $\mu = Q/2$ (dashed line), NNLO $\mu = 2Q$ (dotted line).

**Fig. 10a.** The polarized quantity $N(\mu/\mu_0)$ (Eq. (4.4)) plotted in the range $0.4 < \mu/\mu_0 < 2$ with $Q = 5$ GeV and $\mu_0 = Q$. The results are shown for LO (dotted line), NLO (dashed line), NNLO (solid line).

**Fig. 10b.** Same as in Fig. 10a but now for $Q = 10$ GeV.

**Fig. 10c.** Same as in Fig. 10a but now for $Q = 15$ GeV.

**Fig. 11a.** The unpolarized quantity $N(\mu/\mu_0)$ (Eq. (4.4)) plotted in the range $0.4 < \mu/\mu_0 < 2$ with $Q = 5$ GeV and $\mu_0 = Q$. The results are shown for LO (dotted line), NLO (dashed line), NNLO (solid line).

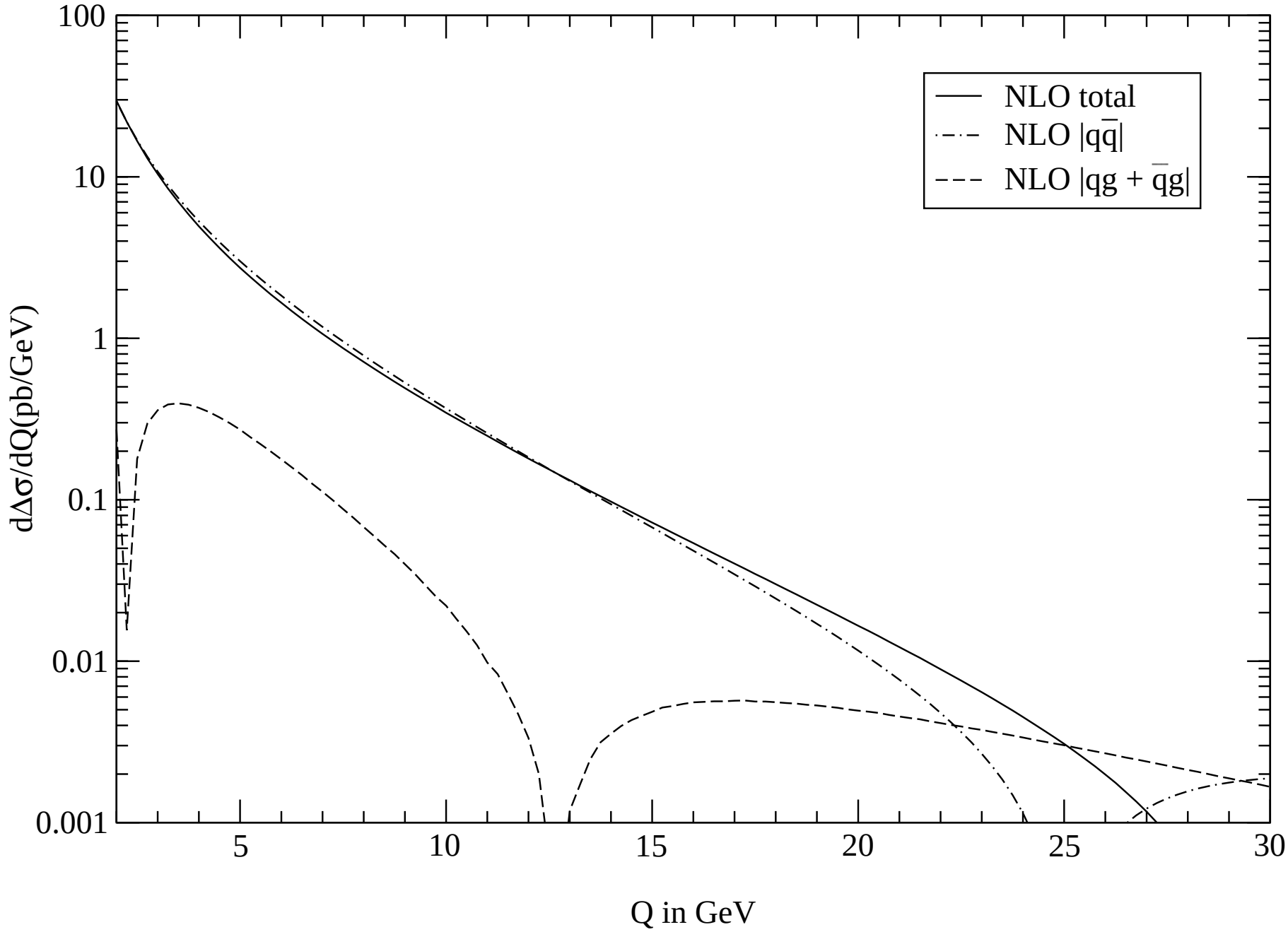
**Fig. 11b.** Same as in Fig. 11a but now for $Q = 10$ GeV.

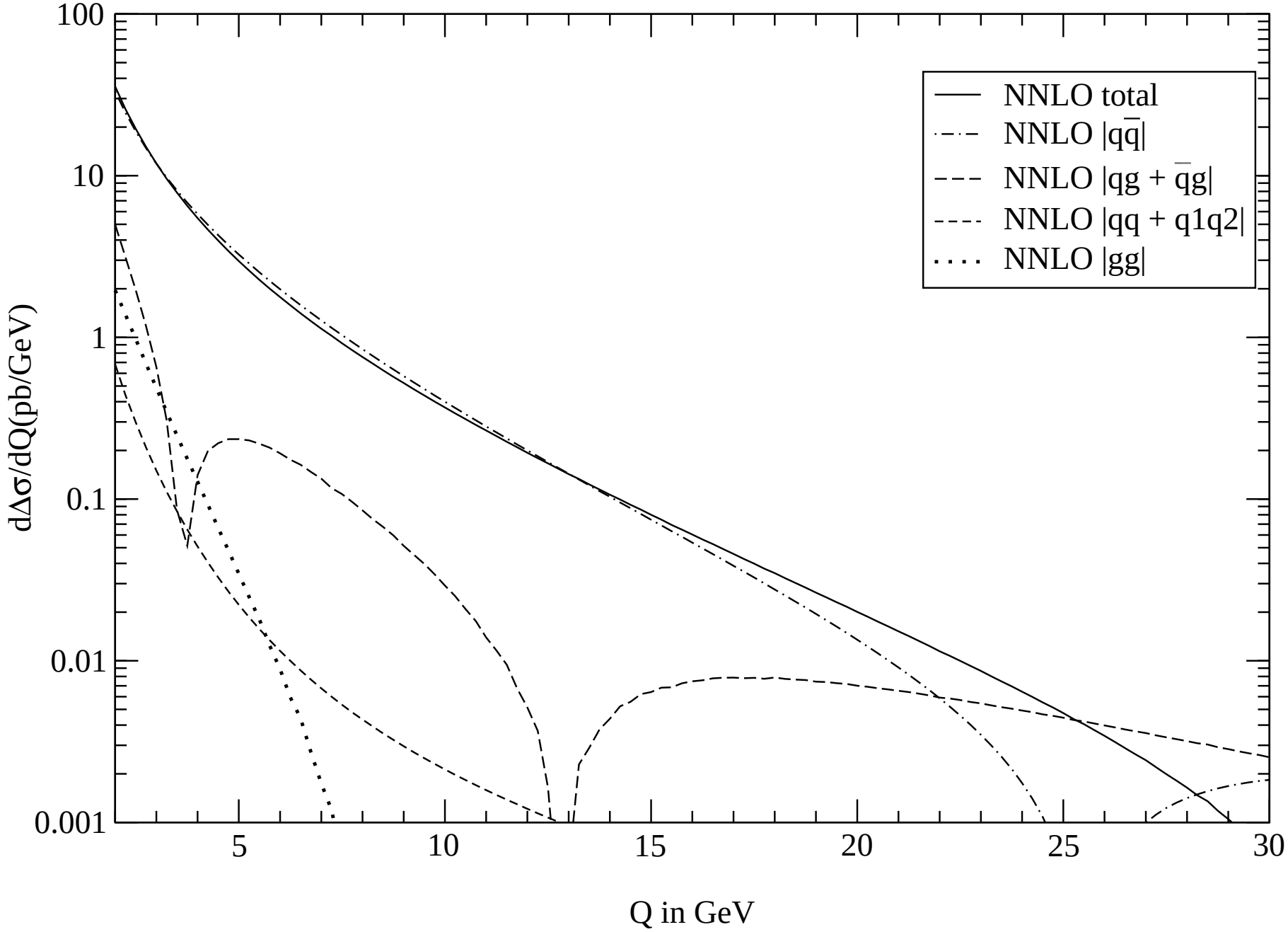
**Fig. 11c.** Same as in Fig. 11a but now for $Q = 15$ GeV.

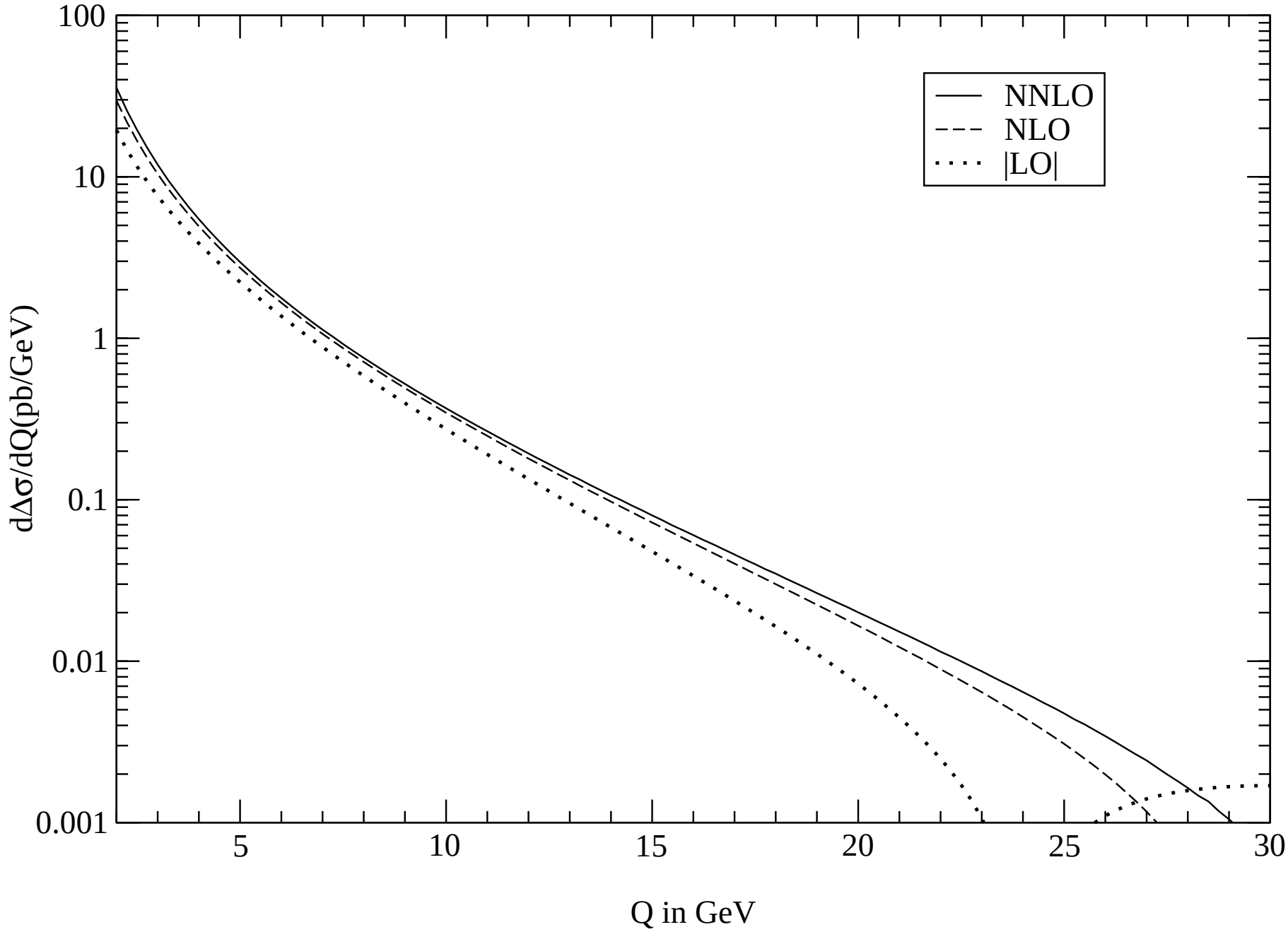
**Fig. 12.** The longitudinal asymmetry $A_{\rm LL}$ (Eq. (4.5)) in % plotted in the range $2 < Q < 30$ GeV at $\mu = Q$. LO (dotted line), NLO (dashed line), NNLO (solid line).

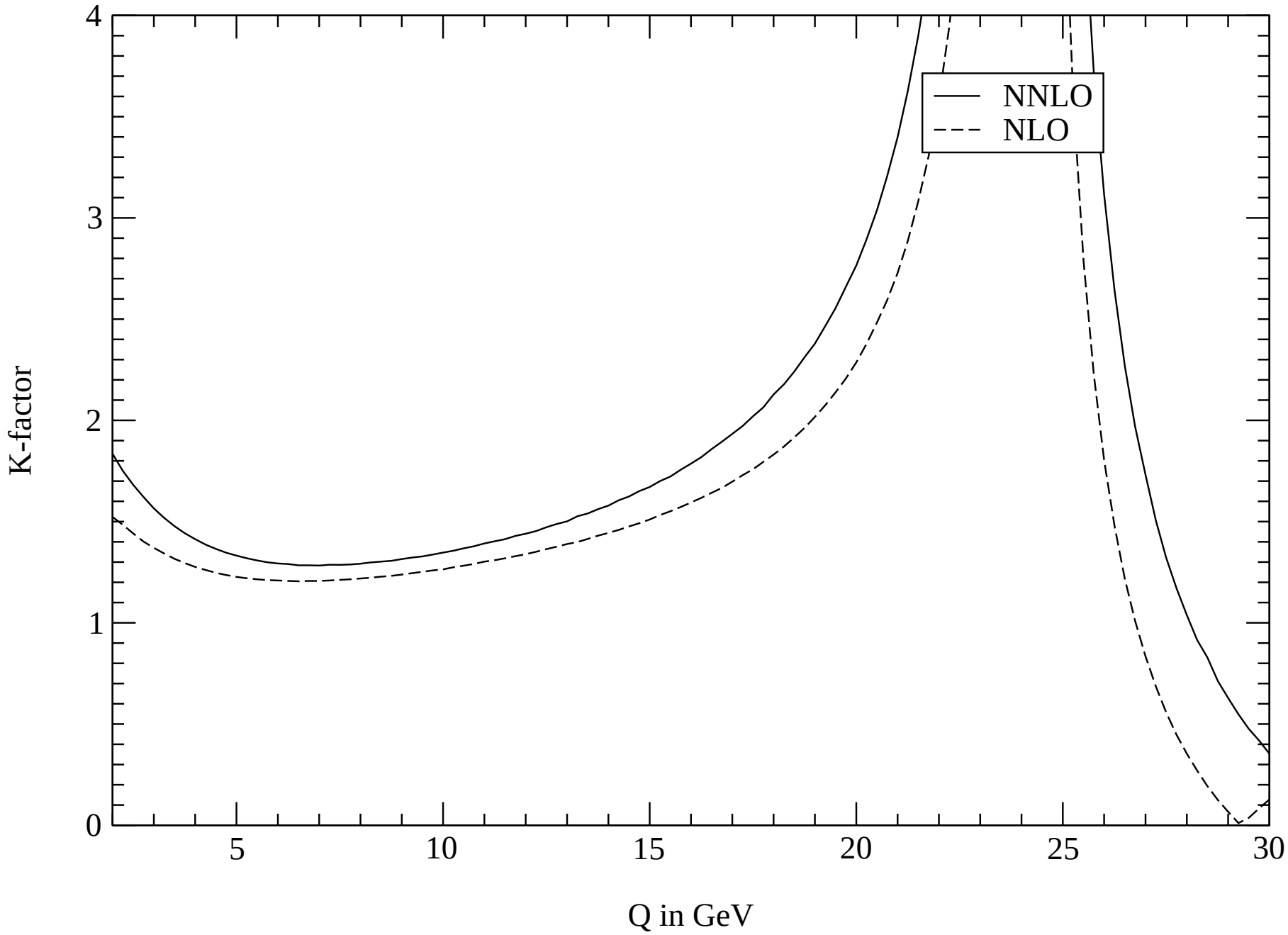
**Fig. 13.** The longitudinal asymmetry $A_{\rm LL}$ (Eq. (4.5)) in % plotted in the range $2 < Q < 30$ GeV at $\mu = Q$ and NLO. BB1 (solid line), BB2 (dot-dashed line), GRVS01, standard scenario (dashed line), GRSV01, valence scenario (dotted line).

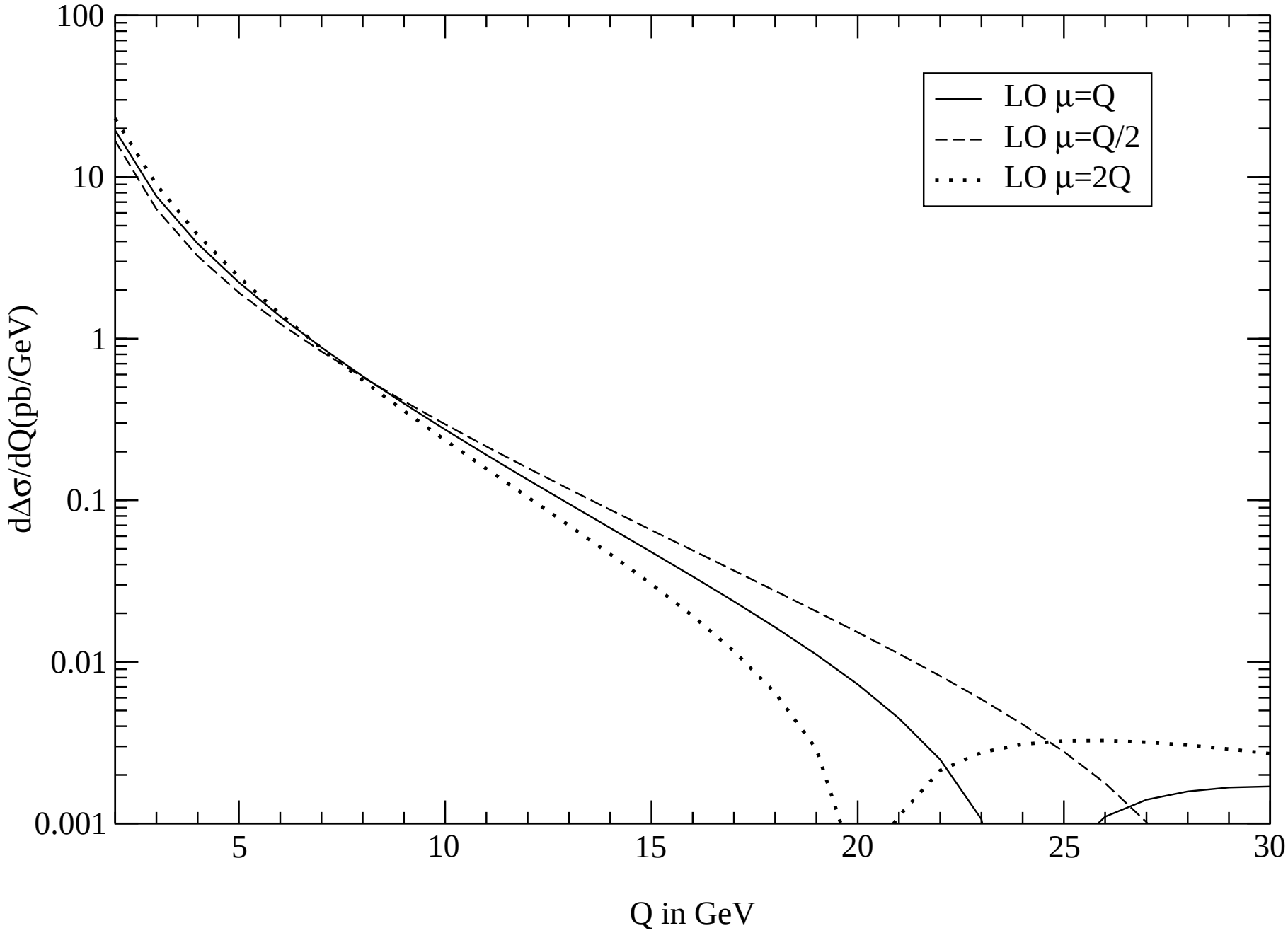
**Fig. 14.** The longitudinal asymmetry $A_{\rm LL}$ (Eq. (4.5)) in % plotted in the range $2 < Q < 30$ GeV at $\mu = Q$ and NNLO. BB1 (solid line), BB2 (dot-dashed line), GRVS01, standard scenario (dashed line), GRSV01, valence scenario (dotted line).

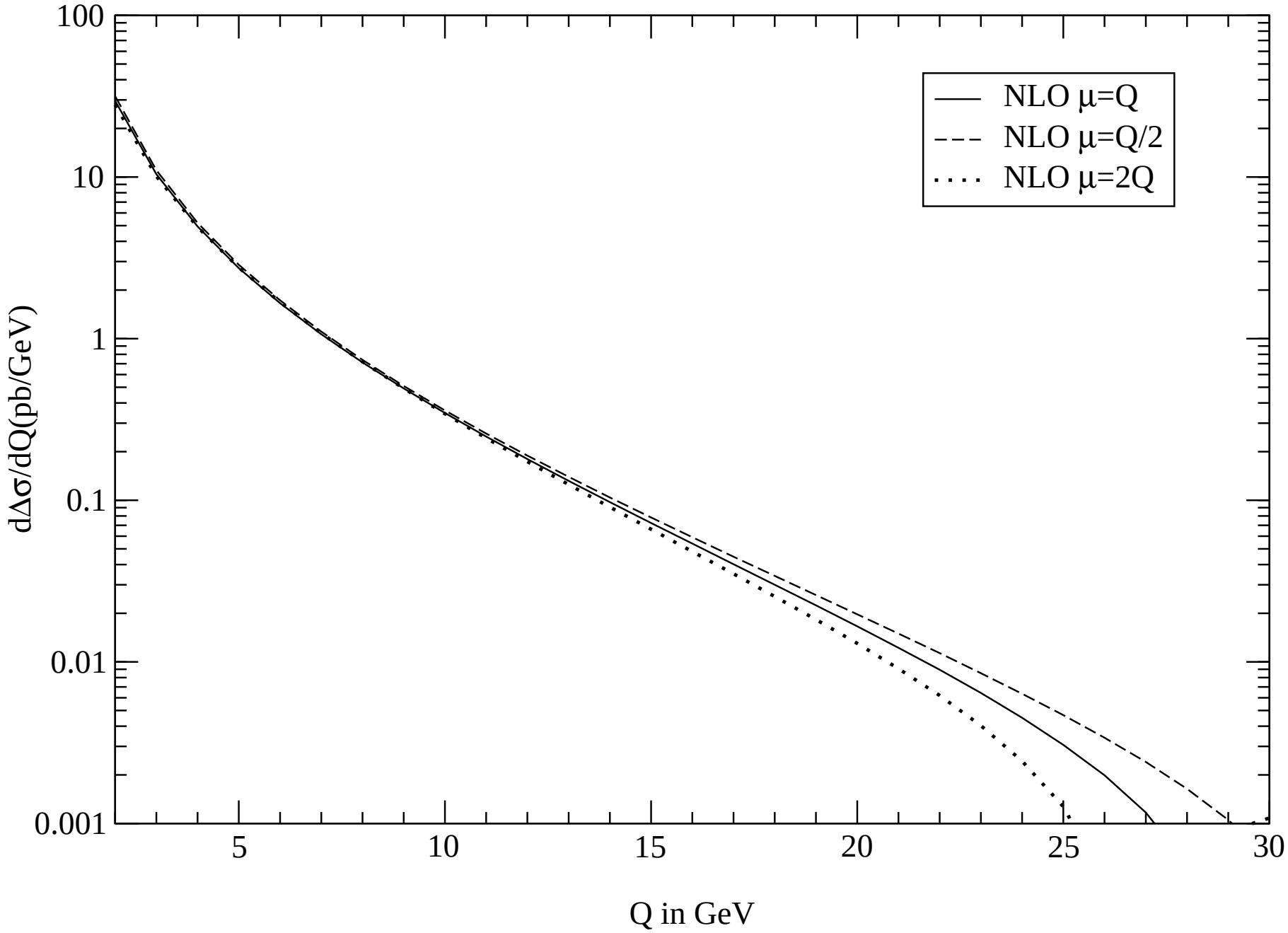

100
10
1
0.1
0.01
0.001
dΔσ/dQ(pb/GeV)
5
10
15
20
25
30
Q in GeV
NLO total
NLO |qq̄|
NLO |qg + q̄g|

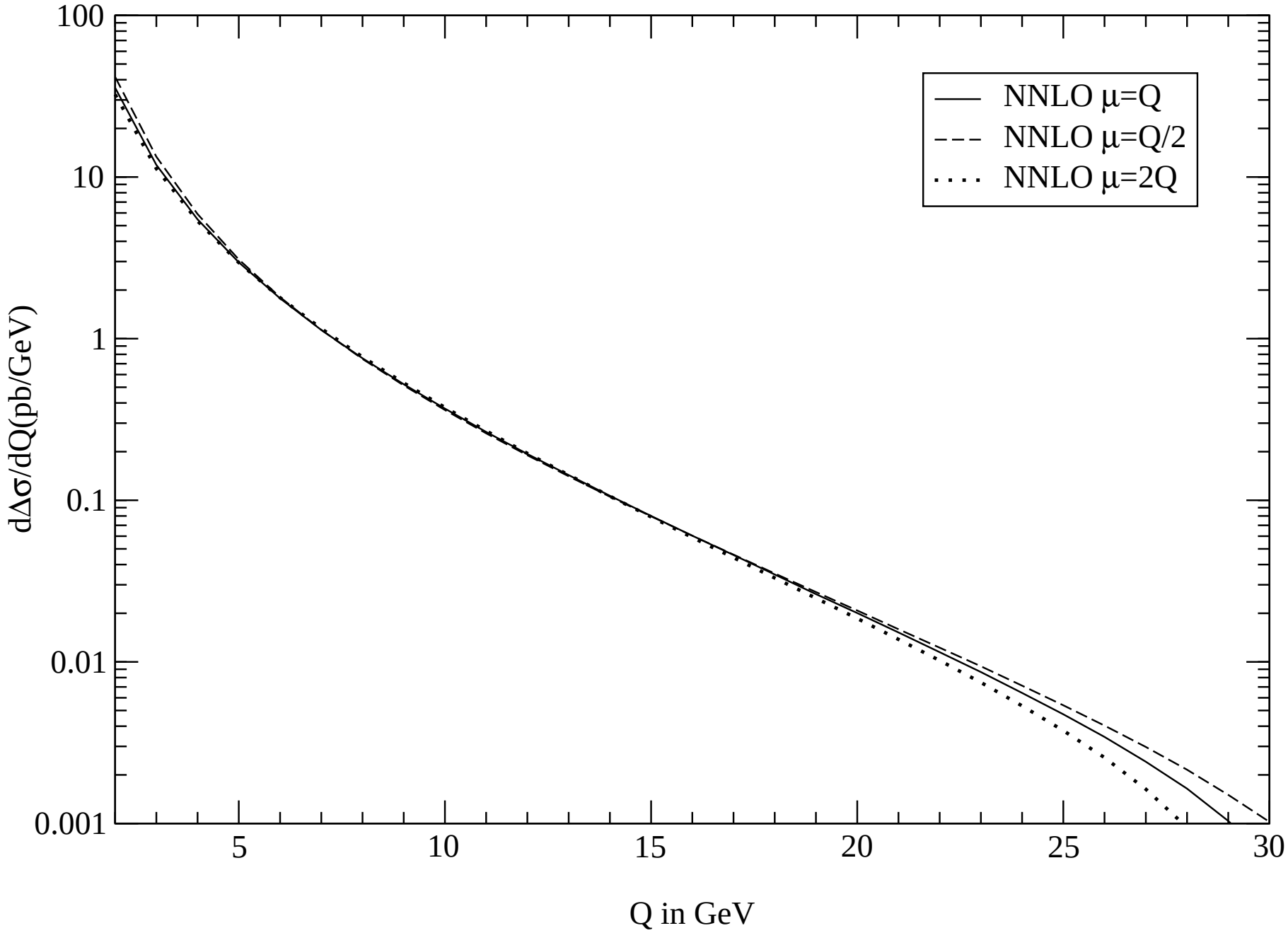

NNLO total
NNLO |qq̄|
NNLO |qg + q̄g|
NNLO |qq + q1q2|
NNLO |gg|
dΔσ/dQ(pb/GeV)
Q in GeV
100
10
1
0.1
0.01
0.001
5
10
15
20
25
30

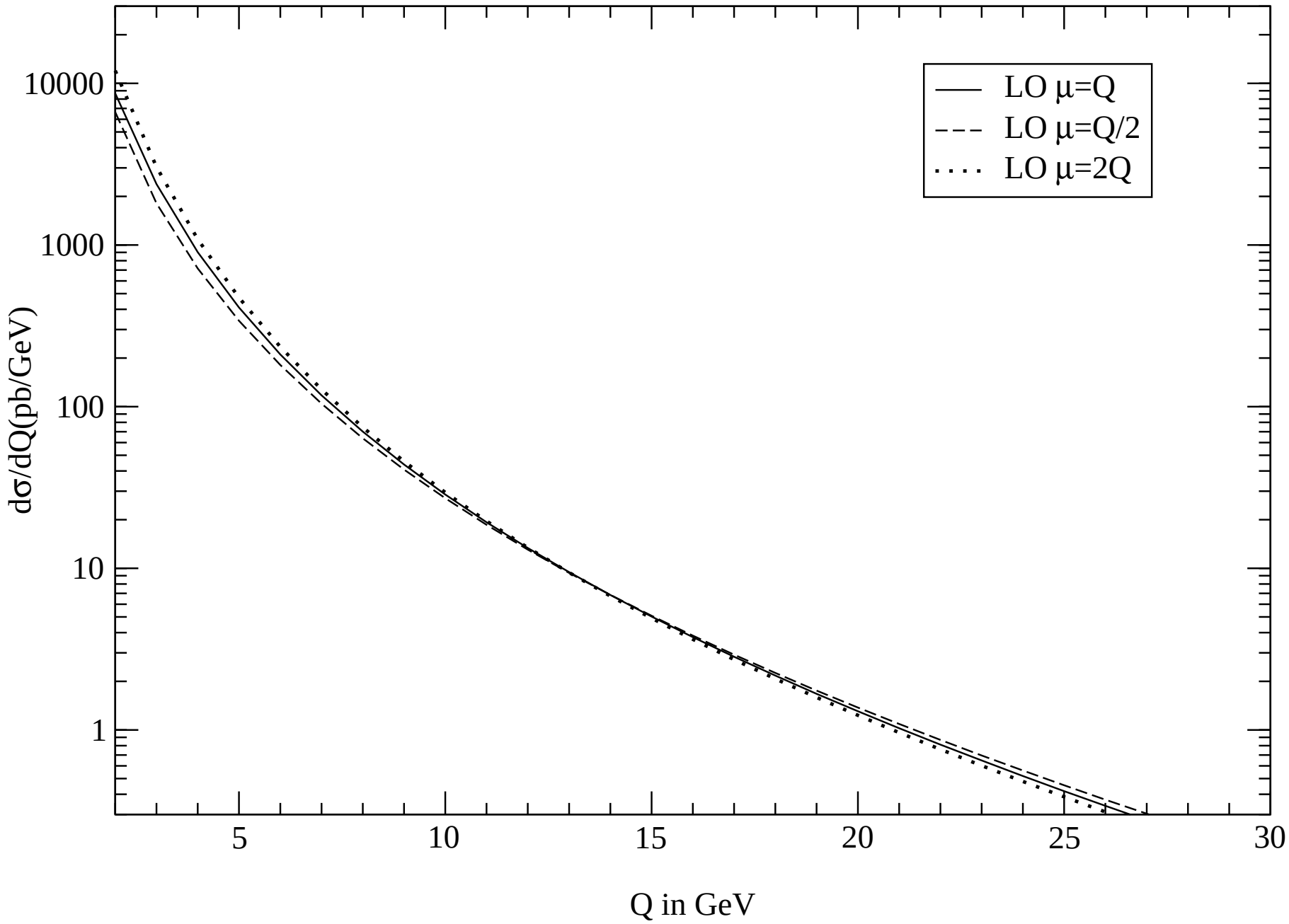

100
10
1
0.1
0.01
0.001
5
10
15
20
25
30
dΔσ/dQ(pb/GeV)
Q in GeV
NNLO
NLO
|LO|

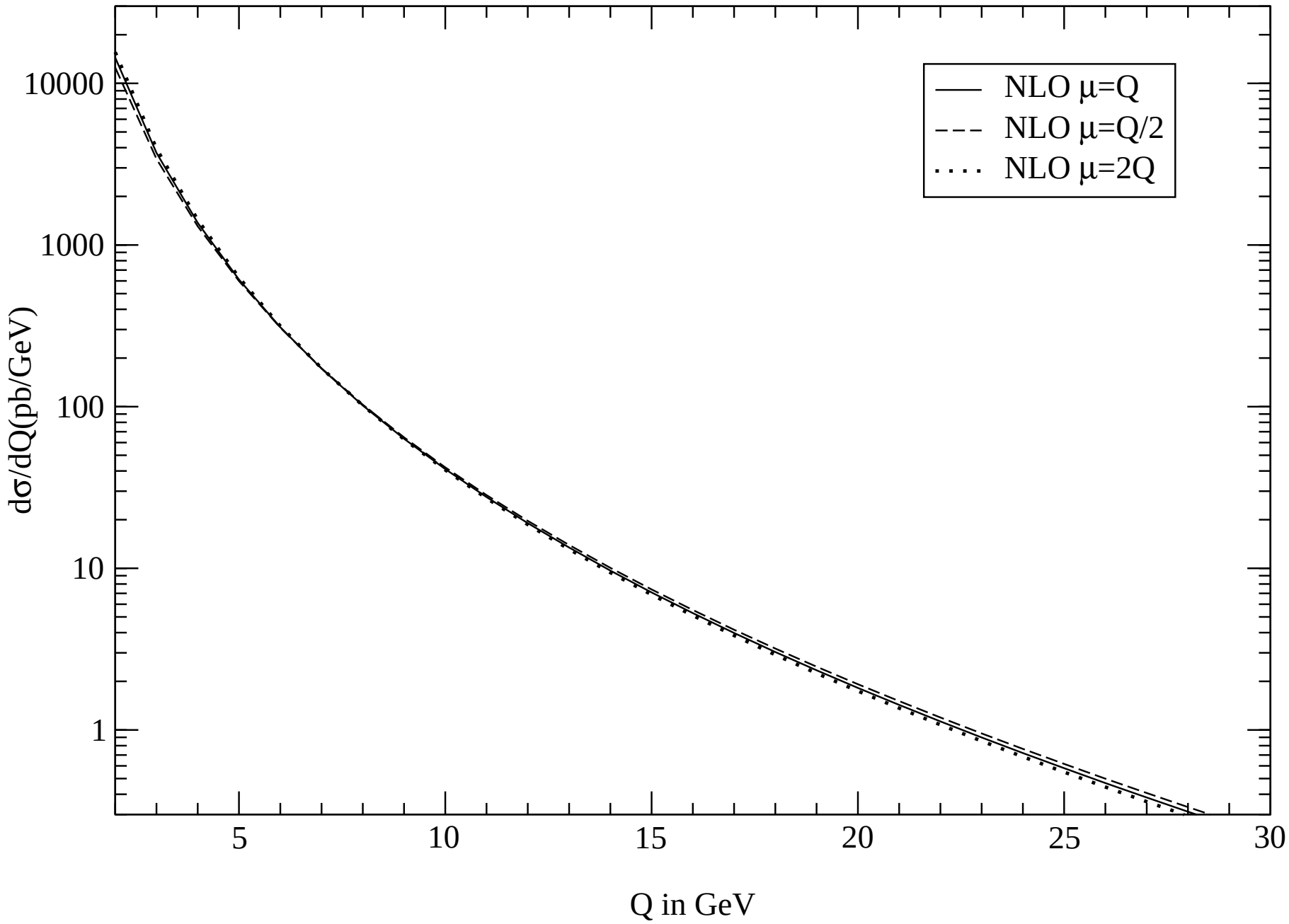

NNLO
NLO
K-factor
Q in GeV
0
1
2
3
4
5
10
15
20
25
30

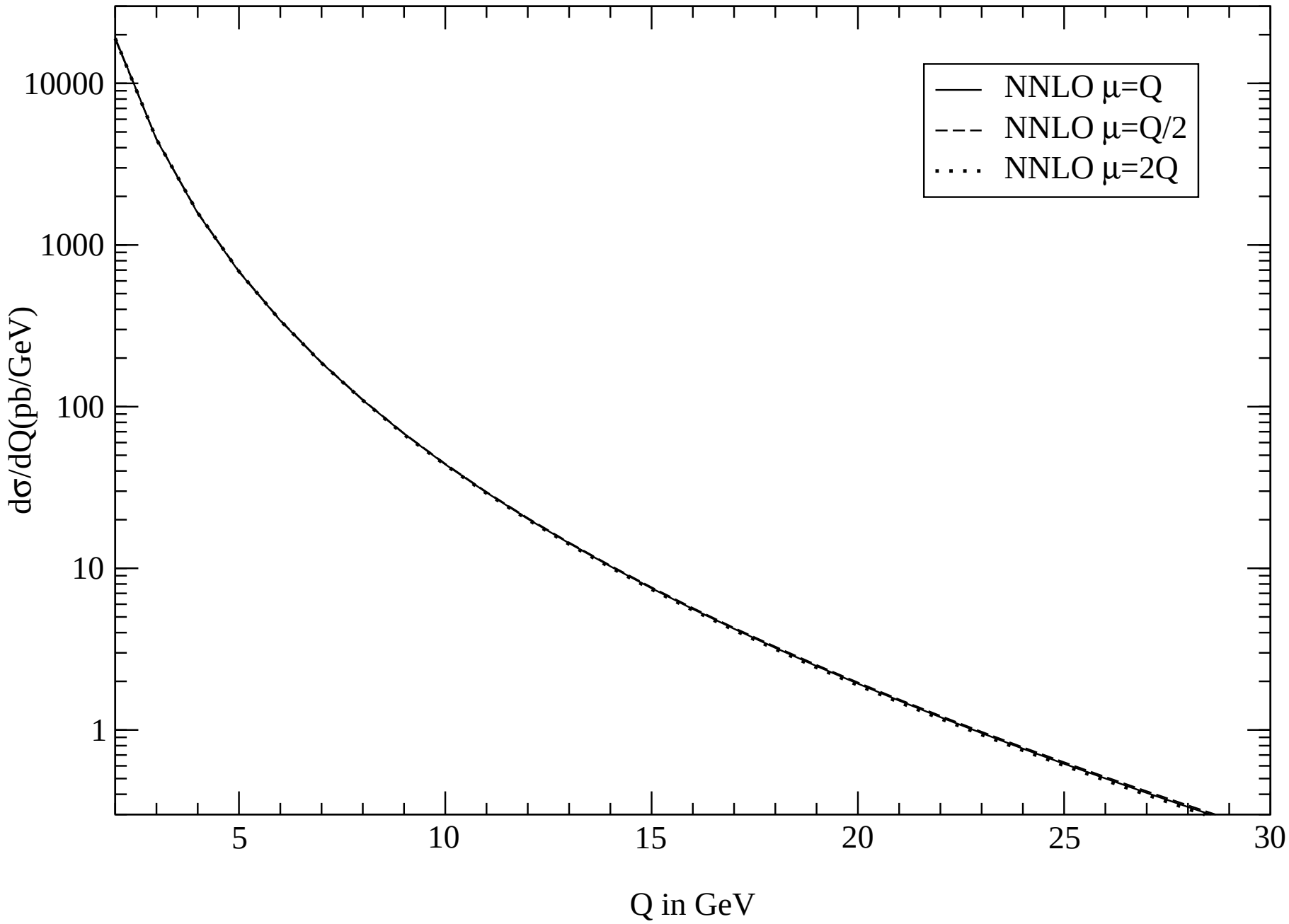

100
10
1
0.1
0.01
0.001
dΔσ/dQ(pb/GeV)
5
10
15
20
25
30
Q in GeV
LO μ=Q
LO μ=Q/2
LO μ=2Q

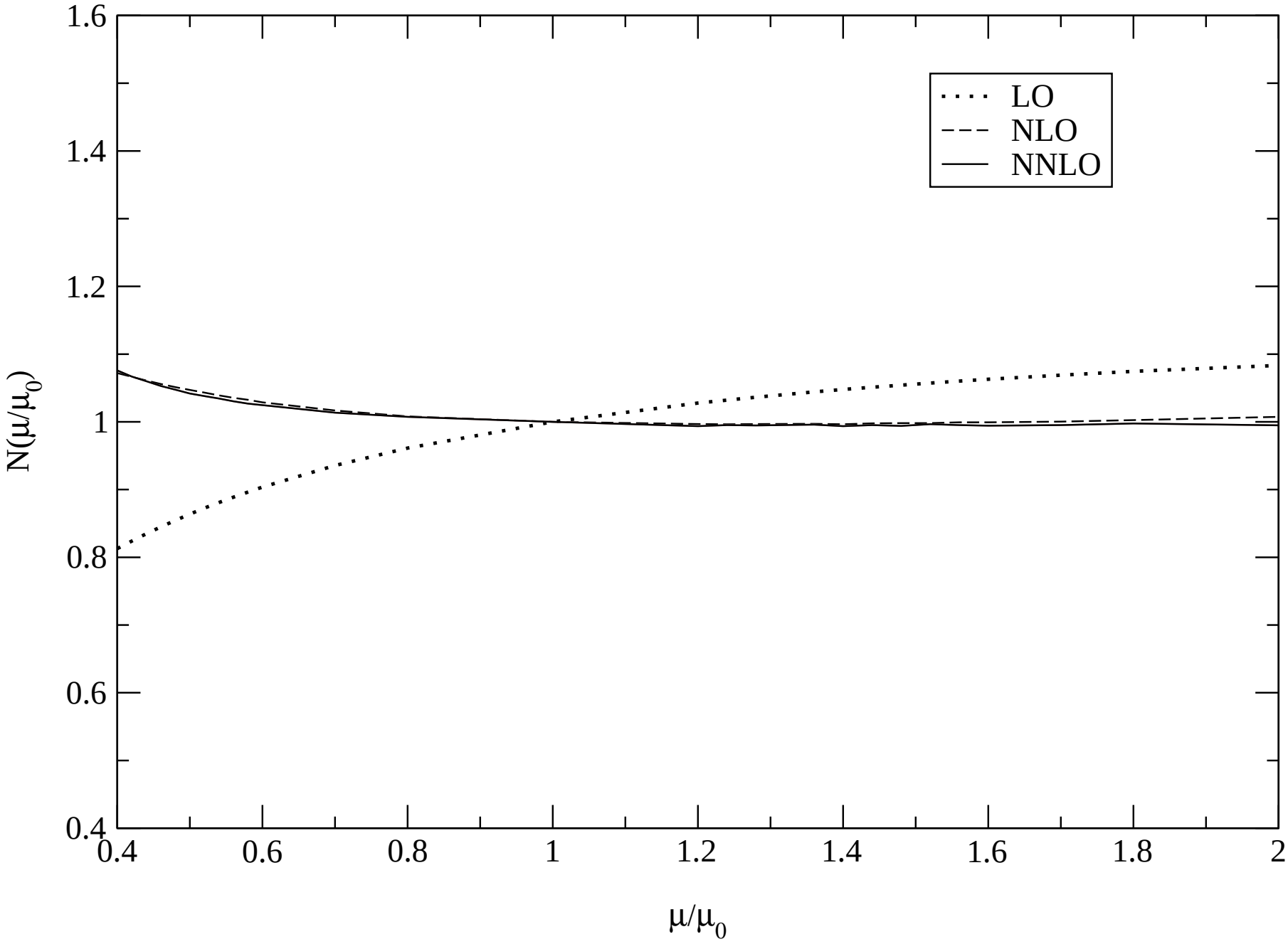

100
10
1
0.1
0.01
0.001
5
10
15
20
25
30
dΔσ/dQ(pb/GeV)
Q in GeV
NLO μ=Q
NLO μ=Q/2
NLO μ=2Q

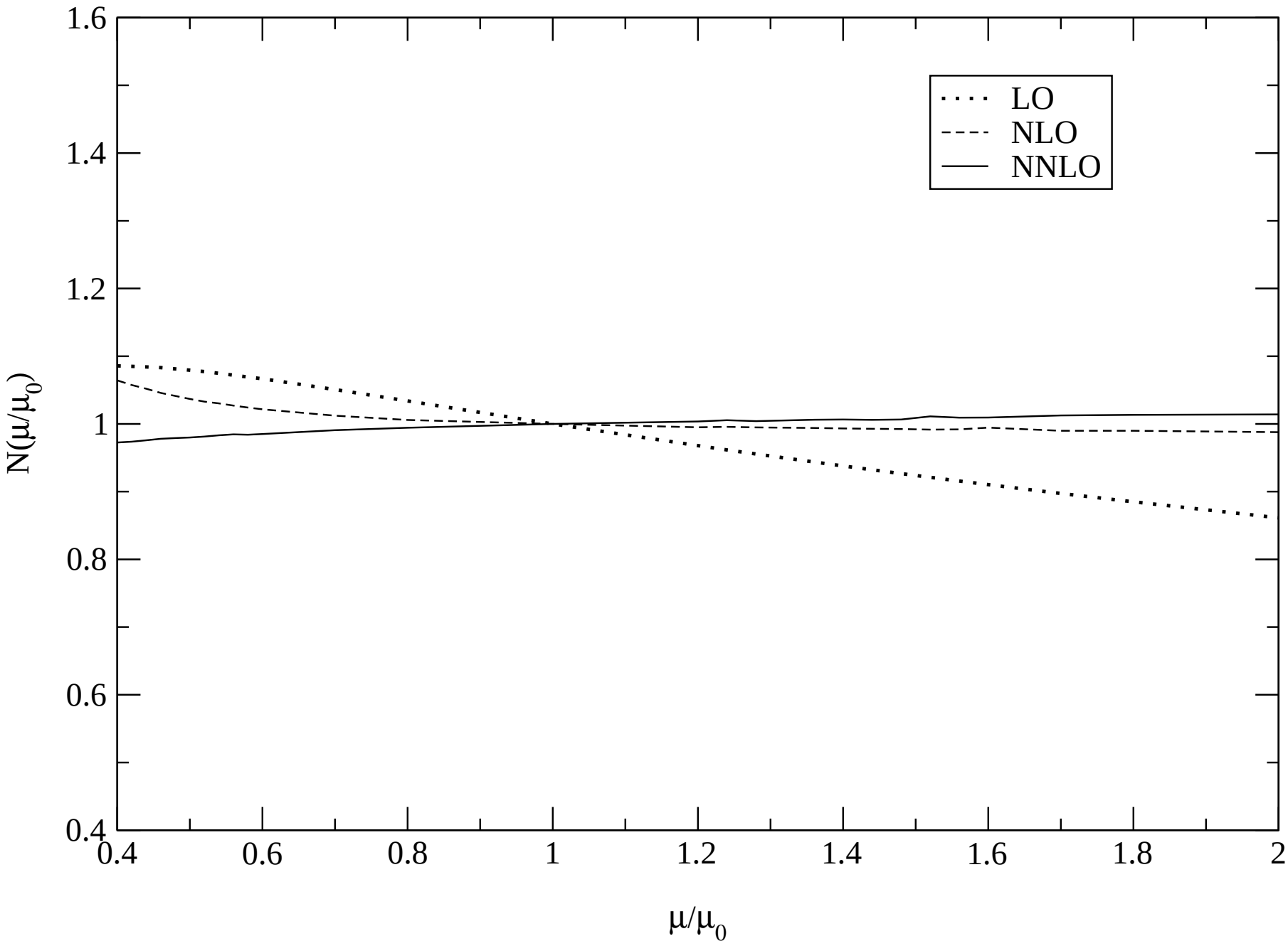

100
10
1
0.1
0.01
0.001
5
10
15
20
25
30
dΔσ/dQ(pb/GeV)
Q in GeV
NNLO μ=Q
NNLO μ=Q/2
NNLO μ=2Q

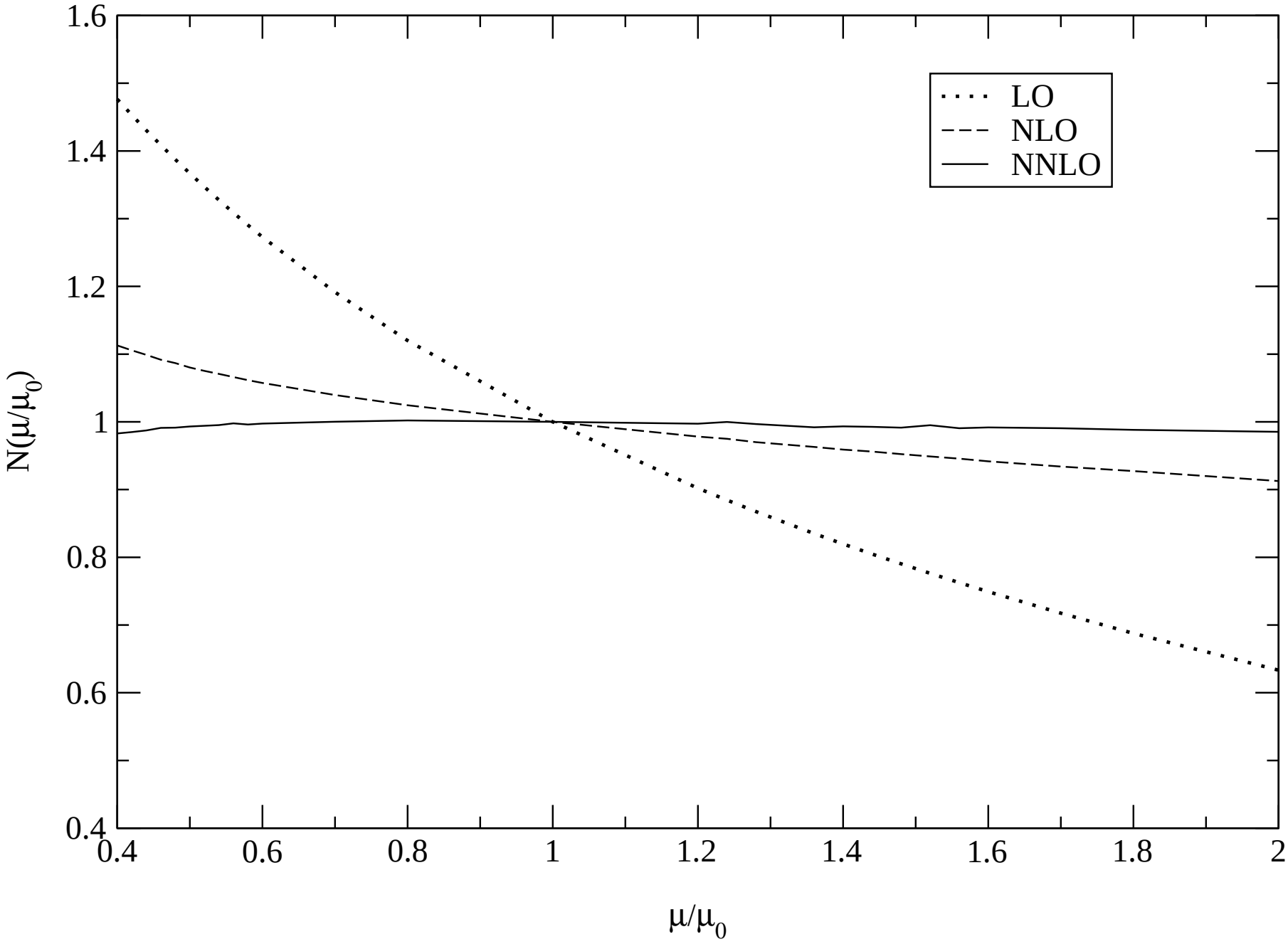

LO μ=Q
LO μ=Q/2
LO μ=2Q
dσ/dQ(pb/GeV)
10000
1000
100
10
1
5
10
15
20
25
30
Q in GeV

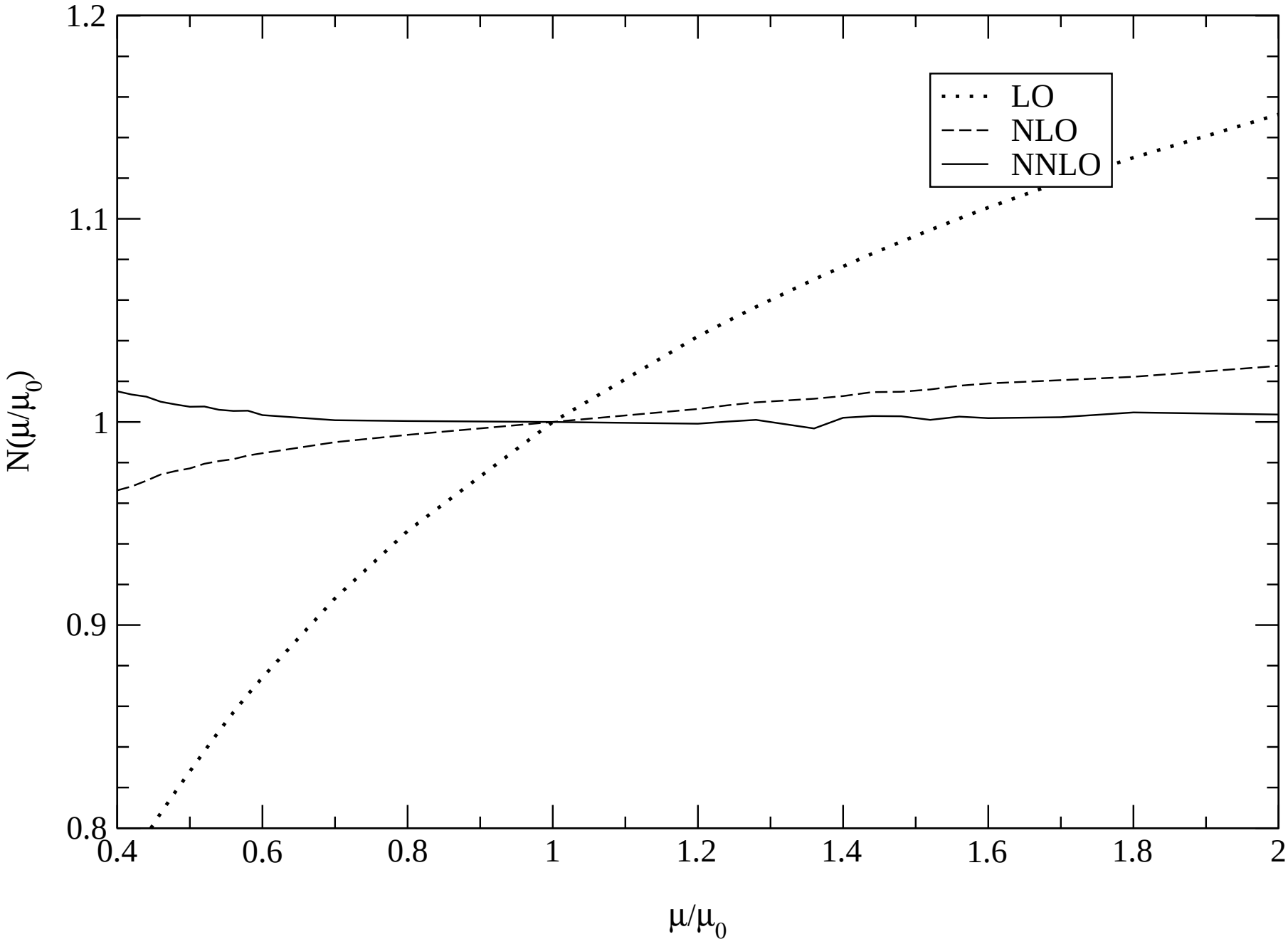

NLO μ=Q
NLO μ=Q/2
NLO μ=2Q
dσ/dQ(pb/GeV)
10000
1000
100
10
1
5
10
15
20
25
30
Q in GeV

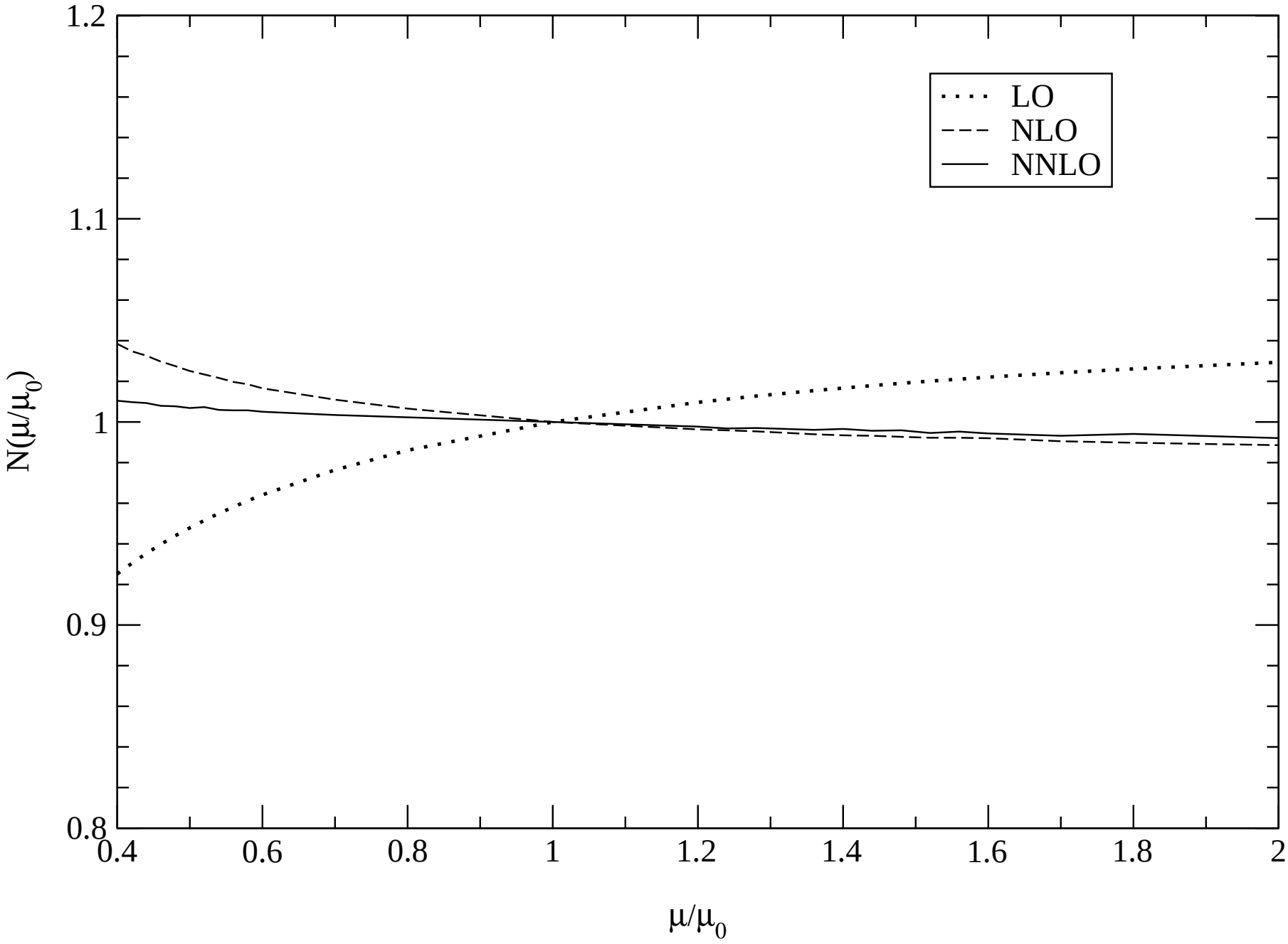

NNLO μ=Q
NNLO μ=Q/2
NNLO μ=2Q
dσ/dQ(pb/GeV)
10000
1000
100
10
1
5
10
15
20
25
30
Q in GeV

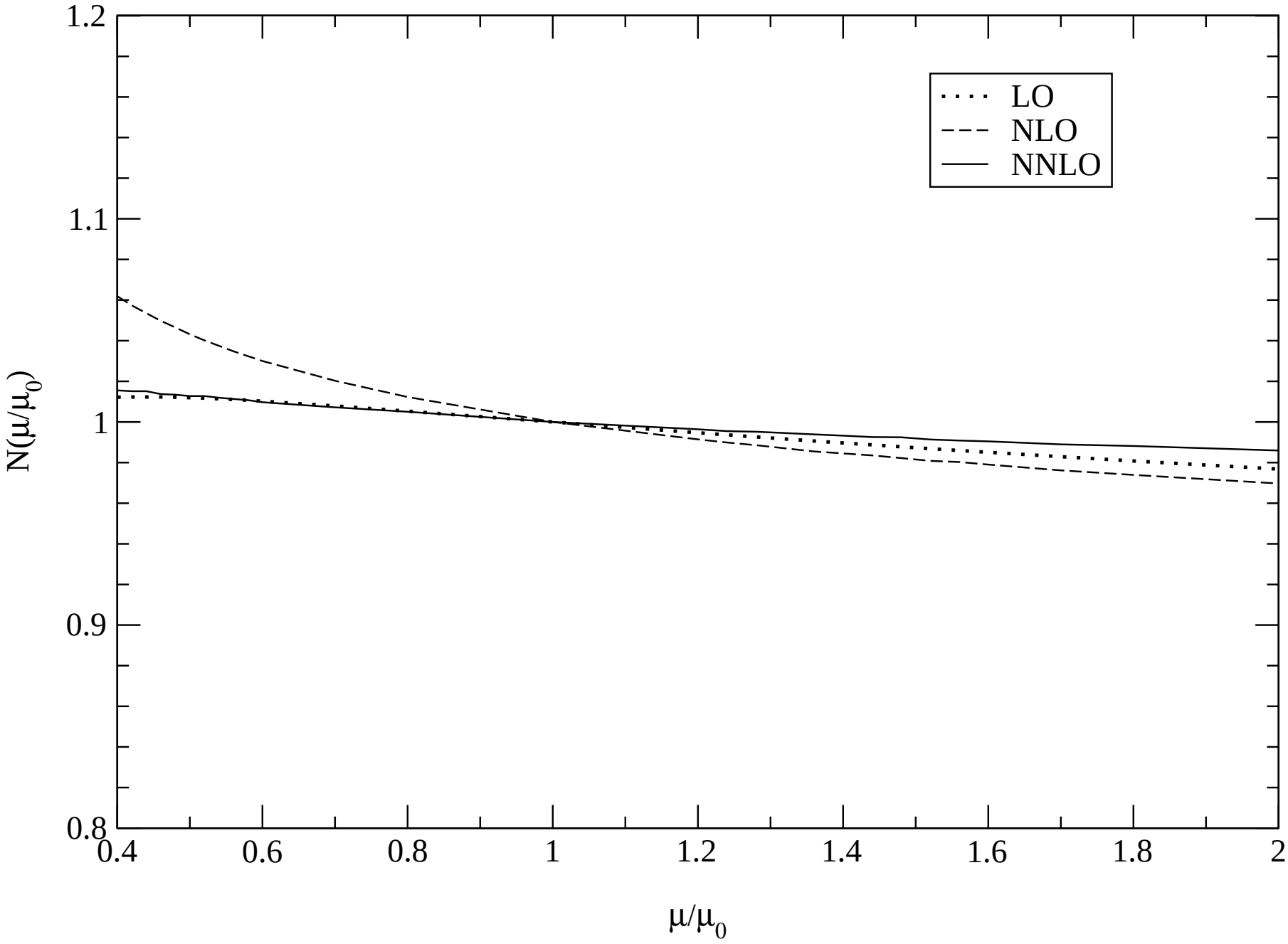

LO
NLO
NNLO
1.6
1.4
1.2
1
0.8
0.6
0.4
0.4
0.6
0.8
1
1.2
1.4
1.6
1.8
2
N(μ/μ0)
μ/μ0

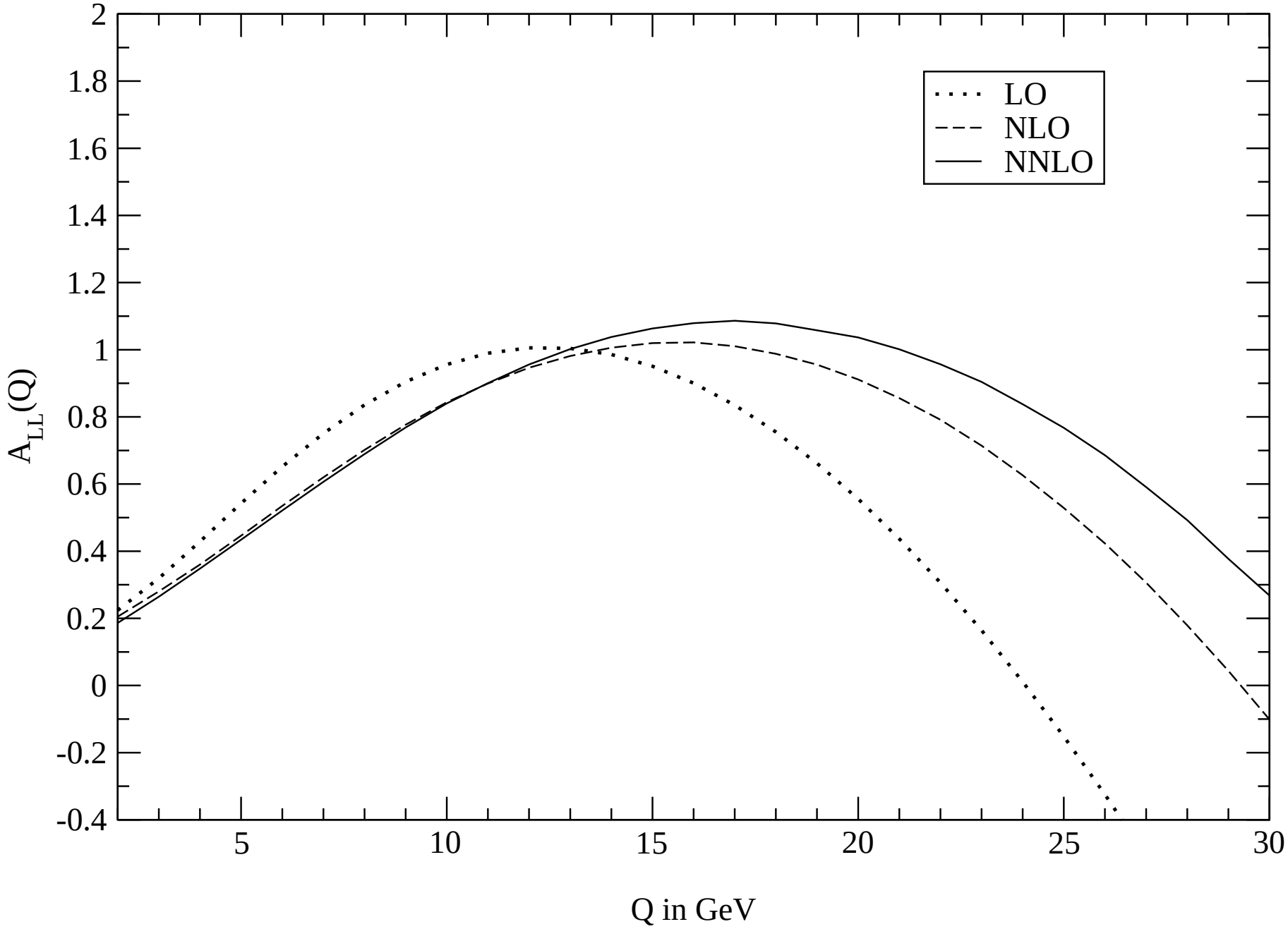

LO
NLO
NNLO
1.6
1.4
1.2
1
0.8
0.6
0.4
0.4
0.6
0.8
1
1.2
1.4
1.6
1.8
2
N(μ/μ0)
μ/μ0

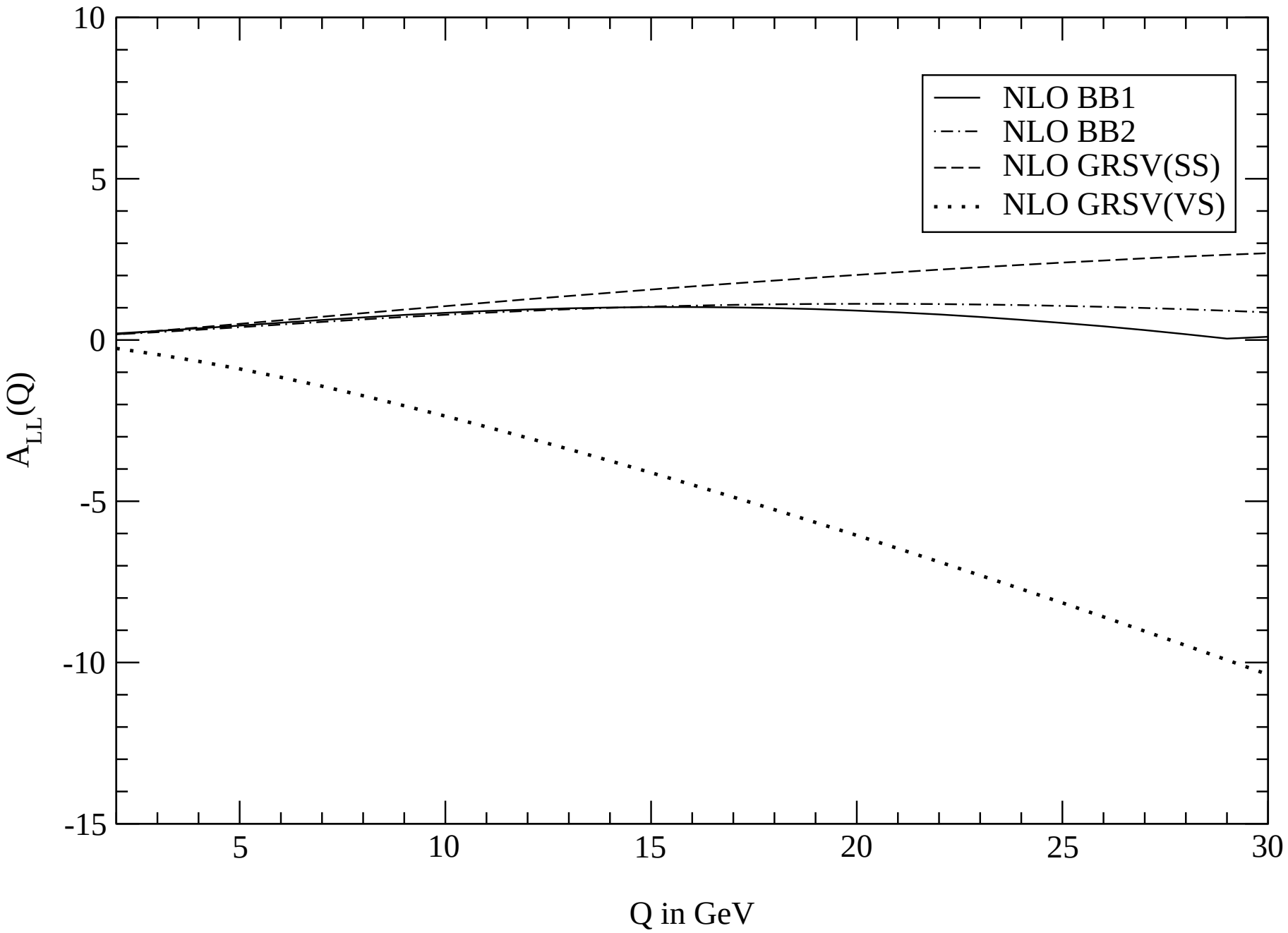

LO
NLO
NNLO
1.6
1.4
1.2
1
0.8
0.6
0.4
0.4
0.6
0.8
1
1.2
1.4
1.6
1.8
2
N(μ/μ0)
μ/μ0

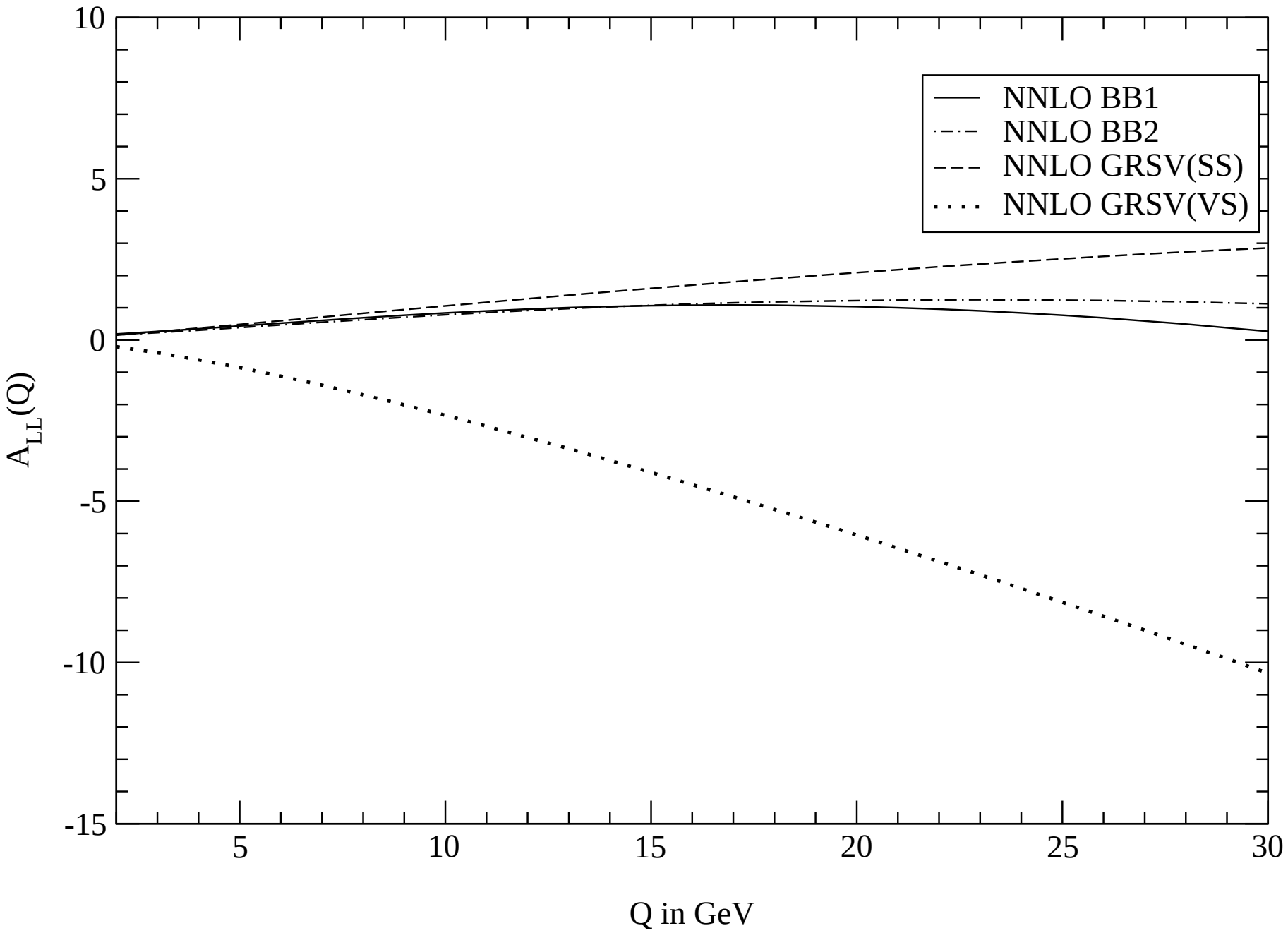

LO
NLO
NNLO
1.2
1.1
1
0.9
0.8
0.4
0.6
0.8
1
1.2
1.4
1.6
1.8
2
N(μ/μ0)
μ/μ0


LO
NLO
NNLO
1.2
1.1
1
0.9
0.8
0.4
0.6
0.8
1
1.2
1.4
1.6
1.8
2
N(μ/μ0)
μ/μ0


LO
NLO
NNLO
1.2
1.1
1
0.9
0.8
0.4
0.6
0.8
1
1.2
1.4
1.6
1.8
2
N(μ/μ0)
μ/μ0


LO
NLO
NNLO
$A_{LL}(Q)$
Q in GeV
2
1.8
1.6
1.4
1.2
1
0.8
0.6
0.4
0.2
0
-0.2
-0.4
5
10
15
20
25
30


NLO BB1
NLO BB2
NLO GRSV(SS)
NLO GRSV(VS)
10
5
0
-5
-10
-15
5
10
15
20
25
30
$A_{LL}(Q)$
Q in GeV


NNLO BB1
NNLO BB2
NNLO GRSV(SS)
NNLO GRSV(VS)
10
5
0
-5
-10
-15
5
10
15
20
25
30
$A_{LL}(Q)$
Q in GeV